# Atmospheric oxygen in the 1990s from a global flask sampling network: Trends and variability pertaining to the carbon cycle

Andrew C. Manning[1]
Ralph F. Keeling
William J. Paplawsky
Laura E. Katz
Elizabeth M. McEvoy
Chris G. Atwood

DRAFT #8: 29-Jan-2003

Scripps Institution of Oceanography, La Jolla, California, USA.

[1] Now at: Max-Planck-Institute for Biogeochemistry, Jena, Germany.

## Abstract.

We present time series measurements of up to 11 years in length of atmospheric $O_2$ and $CO_2$ concentration data from eleven sampling stations worldwide. We discuss the temporal and spatial distributions of the seasonal cycles, interannual long-term trends, and latitudinal gradients observed. With these data we are able to distinguish between oceanic and land biotic carbon uptake and thus we discuss the temporal and spatial variability observed due to processes occurring in these two reservoirs.

From a subset of these data we have calculated a global carbon budget for the decade of the 1990s. Fossil fuel combustion during this period released an average of 6.33±0.38 Gt C/y, of which 3.21±0.13 Gt C/y remained in the atmosphere, 1.68±0.52 Gt C/y were taken up by the oceans, and 1.44±0.66 Gt C/y were taken up by the land biota, illustrating that the land biota and oceans are roughly equally important for global carbon uptake. We repeated this computational technique on shorter one year time-steps, and observed significant interannual variability particularly, in the land biotic carbon sink. El Niño effects appear to play a role in the land biotic sink, but they do not appear to affect the oceanic sink. Other mechanisms remain to be found to explain much of the observed variability. Temporal variability was also observed in the amplitude of the seasonal cycle of $O_2$, and we speculate that in the mid to high latitudes of the southern hemisphere, this results from variability in wind strength over the oceans.

## 1. Introduction

Evidence continues to grow supporting significant anthropogenic-induced changes in Earth's climate system [e.g. *Mann et al.*, 1998; *Tans et al.*, 1996]. One of the major players causing such changes is changes in atmospheric $CO_2$ concentrations, owing to the ability of $CO_2$ to close a portion of the otherwise open absorption window in the radiation spectrum, at 12-17 μm [*Peixoto and Oort*, 1992], preventing infrared radiation from escaping back into space, thus potentially warming the Earth [*Graedel and Crutzen*, 1993]. As anthropogenic $CO_2$ production continues to accelerate from the combustion of fossil fuels it becomes increasingly important to understand the partitioning of $CO_2$ into the atmospheric, oceanic, and terrestrial reservoirs so that reliable future projections of climate and climate change can be made.

Careful measurements of background atmospheric $CO_2$ concentrations from a large number of monitoring stations around the world provide us with spatial and temporal data on the increase of $CO_2$ in the atmospheric reservoir [e.g. *GLOBALVIEW-CO2*, 1999]. But to quantify the partitioning of $CO_2$ uptake in the oceanic and terrestrial reservoirs no direct methods exist, but several different indirect carbon-based methods have been employed, including: use of surface ocean $pCO_2$ data [*Takahashi et al.*, 1999; *Tans et al.*, 1990]; several different approaches making use of atmospheric $^{13}CO_2/^{12}CO_2$ data [*Bacastow et al.*, 1996; *Gruber and Keeling*, 1999; *Heimann and Maier-Reimer*, 1996; *Quay et al.*, 1992; *Tans et al.*, 1993]; use of inverse atmospheric transport models [*Enting et al.*, 1995; *Keeling et al.*, 1989; *Tans et al.*, 1990]; and use of ocean carbon models [several models are compared in *Orr*, 1997]. Each of these methods has inherent strengths and weaknesses. The oceanic $pCO_2$ method suffers from a sparsity of data, particularly in the southern hemisphere, and from uncertainties in gas transfer velocities [*Liss and Merlivat*, 1986]. $^{13}CO_2/^{12}CO_2$ methods make use of the fact that during terrestrial photosynthesis uptake of carbon favors the lighter $^{12}C$ isotope whereas discrimination between the two isotopes in oceanic carbon uptake is very small [*Ciais et al.*, 1995]. Interpreting $^{13}C/^{12}C$ data is complicated, however, by a disequilibrium effect, arising because land biotic respiration occurs from carbon stocks that were assimilated up to several decades earlier. In addition, $C_3$ and $C_4$ plants discriminate against $^{13}C$ to differing degrees and the global relative distributions of $C_3$ and $C_4$ plants, especially in the tropics, is not well known, and changes with time. These methods also suffer from laboratory intercalibration problems. *Heimann and Maier-Reimer* [1996] showed that even with a factor of two reduction in the largest uncertainties in these $^{13}C$ methods, the uncertainty in the oceanic carbon sink would still be 0.8 Gt C/y or greater.

Atmospheric oxygen measurements provide an additional, independent ocean/land carbon sink partitioning method as first discussed by *Machta* [1980], and they can also provide additional information about the global carbon cycle not obtainable from a study of carbon and its isotopes alone [e.g. *Bender et al.*, 1998; *Keeling et al.*, 1993]. $O_2$ and $CO_2$ are inversely linked by the processes of photosynthesis, respiration, and combustion. For example, photosynthesis of land biota produces atmospheric $O_2$ and consumes atmospheric $CO_2$, whereas combustion of fossil fuel or biomass burning consumes $O_2$ and produces $CO_2$. However, several characteristics, all related to oceanic processes, result in decoupled changes in the atmospheric concentrations of $O_2$ and $CO_2$. First, the characteristic most pertinent to distinguishing between the ocean and land partitioning of $CO_2$ is that a portion of the fossil fuel-derived atmospheric $CO_2$ dissolves into the oceans, but the corresponding fossil fuel-derived atmospheric $O_2$ decrease is not offset by an $O_2$ flux from the oceans. This is because in the ocean-atmosphere system, 99% of the $O_2$ is in the atmosphere because $O_2$ is relatively insoluble in seawater [e.g. *Bender and Battle*, 1999], hence the *relative* changes in the atmospheric $O_2$ concentration caused by fossil fuel combustion are very small and result in no appreciable change in the equilibrium position with respect to the ocean. In contrast, only 2% of the carbon in the ocean-atmosphere system is in the atmosphere [e.g. *Bender and Battle*, 1999], thus changes in atmospheric $CO_2$ are relatively significant and perturb the atmosphere-ocean equilibrium, driving a flux of $CO_2$ across the air-sea interface into the oceans.

Second, although biologically-induced seasonal changes in dissolved $O_2$ and dissolved $CO_2$ in the euphotic zone of the ocean are inversely coupled, the air-sea fluxes of these two species are decoupled owing to a $CO_2$ buffering effect created by reactions of $CO_2$ with water to form carbonic acid and carbonate and bicarbonate ions, whereas $O_2$ is geochemically neutral in the oceans. Therefore the partial pressure of dissolved $CO_2$ has a much smaller seasonal variation than it would if $CO_2$ were geochemically neutral, resulting in a much smaller seasonal signal of air-sea gas exchange of $CO_2$.

Third, seasonal $CO_2$ fluxes across the air-sea interface are further suppressed because of the opposing effects of marine biotic photosynthesis and respiration patterns versus temperature-induced solubility changes and mixed-layer depth changes. In autumn and winter, for example, the mixed layer deepens incorporating $CO_2$-rich waters in surface waters and at the same time photosynthesis is less dominant over respiration, combining to increase surface water $CO_2$ concentrations. However, at the same time cooler surface waters result in higher gas solubilities and waters can hold more dissolved $CO_2$ without becoming supersaturated. In contrast, also in autumn and winter, deepening of the mixed layer incorporates $O_2$-depleted waters in surface waters, less photosynthesis produces less $O_2$, and colder waters cause an increase in the undersaturation of $O_2$. These processes combine to drive a net flux of $O_2$ from the atmosphere into the oceans. During spring and summer these effects are opposite with a net $O_2$ flux out of surface waters. In summary, these effects partially cancel each other out for $CO_2$, but reinforce each other for $O_2$, causing an even greater flux of $O_2$ across the air-sea interface and a much weaker $CO_2$ flux. The magnitude of these effects is dependent on latitude and region, but as a very rough estimate, the ocean temperature effects contribute about 15% of the observed atmospheric $O_2$ ratio seasonal cycle.

The fourth difference is similar to the third, but occurs on different spatial and temporal scales. Beneath the seasonal thermocline, in the main thermocline, falling organic matter is respired causing $O_2$ undersaturation. These waters are transported laterally along isopycnal (constant density) surfaces from low latitude waters, where they tend to be deep, to high latitudes where they outcrop and are ventilated. These waters are undersaturated in $O_2$ both because of the respiration of organic matter that occurred at low latitudes and due to the lower temperatures at higher latitudes increasing solubility, therefore they present an $O_2$ demand to the atmosphere. As in the case above, however, these respiration and temperature-solubility effects cancel for $CO_2$. These lateral, main thermocline ocean ventilation processes occur on decadal time scales.

Finally, for processes on land, although $O_2$ and $CO_2$ are always inversely coupled, different processes have different $O_2$:$CO_2$ molar exchange ratios and thus can be distinguished from each other. Fossil fuel combustion has a global average $O_2$:$CO_2$ exchange ratio of about 1.39 moles of $O_2$ consumed per mole of $CO_2$ produced [*Keeling*, 1988a], whereas land biotic photosynthesis and respiration has an average ratio of about 1.1 [*Severinghaus*, 1995]. These ratios can vary over spatial and temporal scales, for example in regions with high natural gas usage such as The Netherlands values greater than 1.5 have been observed (H. Meijer, personal communication), whereas a study of diurnal cycling at the WLEF tower in Wisconsin, USA, has shown ratios as low as 0.97.

For a more in-depth discussion of the physical, chemical and biological controls and influences on atmospheric $O_2$ concentrations, the reader is referred to *Bender and Battle* [1999] and *Bender et al.* [1998].

A landmark in early measurements of atmospheric $O_2$ concentrations are those of *Benedict* [1912] who used a chemical extraction technique followed by volumetric analysis. *Benedict* [1912] reported that atmospheric $O_2$ was constant to the precision he could attain of 60 ppm. Subsequent measurements by *Carpenter* [1937] with a similar measurement technique and *Machta and Hughes* [1970] with a paramagnetic technique, reaffirmed *Benedict's* [1912] results to approximately the same level of precision.

More recently, several independent analytical techniques have been developed, some of which can measure atmospheric $O_2$ to a precision of 1 ppm or better. All of these techniques have been used to demonstrate atmospheric $O_2$ variability, and used in the study of biogeochemical processes such as those described above. The techniques that have been developed are interferometric [*Keeling*, 1988b]; zirconium oxide electrode electrochemistry [*Bloom et al.*, 1989]; mass spectrometric [*Bender et al.*, 1994b]; paramagnetic [*Manning et al.*, 1999]; vacuum ultraviolet absorption [*Stephens*, 1999]; gas chromatographic [*Tohjima*, 2000]; and lead electrode fuel cell electrochemistry (B. Stephens, personal communication).

*Keeling and Shertz* [1992] presented the first time series of precise atmospheric $O_2$ measurements, showing data from three years of sampling at three different locations. From these data they calculated oceanic and land biotic carbon sinks, and they gave an estimate of net production in the global ocean derived from the atmospheric $O_2$ seasonal cycles observed. *Keeling et al.* [1996] updated the oceanic and land biotic sinks estimate with three more years of data, and also interpreted the latitudinal gradient of atmospheric $O_2$ concentrations to estimate the hemispheric distribution of the land biotic sink. *Bender et al.* [1996] established an independent sampling program and from their data they calculated independent estimates of the oceanic and land biotic $CO_2$ sinks, and estimates for net oceanic production in the southern hemisphere. In a continuation of the same sampling program, *Battle et al.* [2000] updated the oceanic and land biotic sinks estimate to mid-1997 and compared these results with sinks derived from an analysis of $^{13}CO_2$ data.

In order to estimate oceanic and land biotic $CO_2$ sinks prior to 1989 when atmospheric $O_2$ measurement flask programs first began, *Bender et al.* [1994a] and *Battle et al.* [1996] studied air in the firn of Antarctic ice sheets at Vostok and South Pole respectively. Another analysis of old air was carried out by *Langenfelds et al.* [1999] using the Cape Grim Air Archive, a suite of tanks filled with air samples between 1978 and 1997. Unfortunately, unsuitable sampling techniques meant that most of the samples contained artefacts in $O_2$ concentration, but despite this *Langenfelds et al.* [1999] were able to give an estimate of the oceanic and land biotic sinks for this time period.

Finally, atmospheric $O_2$ measurements have been used to improve our knowledge in other areas of biogeochemical interest. *Keeling et al.* [1998b] used $O_2$ data and an atmospheric transport model to improve estimates of air-sea gas-exchange velocities; *Stephens et al.* [1998] used the same data and transport model to compare and assess the performance of three different ocean carbon cycle models; and *Balkanski et al.* [1999] incorporated satellite ocean color data into an ocean biology model to estimate $O_2$ fluxes, then used an atmospheric transport model to calculate seasonal cycles of atmospheric $O_2$. By comparing to observed $O_2$ seasonal cycles *Balkanski et al.* [1999] were able to assess both the satellite data and the ocean biology model.

The remainder of this paper will update and expand on the results of *Keeling and Shertz*

[1992] and *Keeling et al.* [1996], showing six additional years of data and a larger network of sampling stations. Section 2 describes our flask sampling and analysis methods, presents preliminary data, and discusses various manipulations and omissions we have carried out on the preliminary data, correcting for obvious technical and logistical reasons. Section 3 calculates global oceanic and land biotic carbon sinks for the 1990s, and compares these results against different computational techniques, and with other results published in the literature. Section 4 discusses interannual variability observed in the oceanic and land biotic sinks, in secular trends, in the amplitude of seasonal cycles, and in latitudinal gradients, and discusses possible mechanisms for these observations.

## 2. Sample Collection and Analysis of Preliminary Data

### 2.1. Methods

The eleven field sampling stations in the Scripps $O_2/N_2$ network are shown in Table 1 and Figure 1. Stations were selected in a manner so as to achieve a globally representative network, and taking advantage of previously established sampling stations. Sampling ceased at Niwot Ridge (NWR) in April 1993, shortly after our laboratory was moved from the National Center for Atmospheric Research (NCAR) in Boulder, Colorado to Scripps Institution of Oceanography in La Jolla, California. The Macquarie Island (MCQ) record was obtained for only 17 months before it was stopped in January 1994 because of high shipping costs.

Flask sampling methodology is described in detail in *Keeling et al.* [1998a]. Briefly, ambient air samples are collected at each station approximately biweekly, in triplicate, in 5 L glass flasks equipped with two stopcocks sealed with Viton o-rings. Prior to shipment to field stations, flasks contain dry air at approximately 1 bar. At each station air is drawn through an intake line mounted up a tower or mast. A small compressor pump maintains an air flow ranging from 2 to 5 STP L/min, depending on the station, flushing ambient air through each flask. A cold trap at temperatures ranging from -55°C to -90°C, depending on the station, pre-dries the air to remove water vapour. Flushing continues until a minimum of 15 flask volumes have passed through each flask, then the sample is sealed off, at a pressure of approximately 1 bar. A back pressure regulator is employed at stations located significantly above sea level to achieve 1 bar of pressure in the flasks. Samples are collected in a temperature-controlled environment to minimize possible fractionation effects. Flask samples are shipped back to our laboratory in La Jolla for analysis. In the case of South Pole (SPO) and Macquarie Island, samples may be stored on site for as long as ten months before they are shipped back to La Jolla, and as long as two months at Palmer Station (PSA). All other stations ship samples back within three weeks of collection.

Flask samples are collected by station personnel during what are considered to be “clean, background air” conditions. The general criteria used to determine when these conditions are met is a pre-established wind direction and speed, and where available, relatively steady, non-fluctuating, *in situ* atmospheric $CO_2$ concentrations, or criteria based on other trace gas species which are measured *in situ*. We wish to sample air that has not been contaminated by local or regional anthropogenic or terrestrial processes. In this manner we can observe synoptic and hemispheric-scale spatial trends, and seasonal and interannual temporal trends. Thus, for example, stations such as La Jolla (LJO) and Cape Grim (CGO), require a relatively narrow wind direction window (roughly westerlies for both stations) to meet these sampling requirements. Cape Kumukahi (KUM) and American Samoa (SMO) on the other hand require the prevalent easterly trade winds.

In our laboratory flask samples are analysed simultaneously for $CO_2$ concentration on a Siemens nondispersive infrared analyser (NDIR), and for $O_2/N_2$ ratio on our interferometric analyser [*Keeling*, 1988b]. Samples are analysed relative to a working gas, which in turn is calibrated each day against a pair of secondary reference gases of pre-determined $O_2/N_2$ ratios and $CO_2$ concentrations. A suite of twelve primary reference gases are analysed roughly every six months as a check on the long-term stability of the secondary reference gases for both $O_2/N_2$ ratios and $CO_2$ concentrations. (See *Keeling et al.* [1998a] for a detailed discussion on reference gases and calibration procedures). In early 2000 we updated our long term $O_2/N_2$ and $CO_2$ calibration scales based on observed eleven-year trends of these primary gases, and, for $CO_2$, based on careful comparisons over the same time period against the "Scripps 1999 manometric scale" maintained at the $CO_2$ laboratory of C. D. Keeling at the Scripps Institution of Oceanography.

## 2.2. Preliminary Data Presentation

Figures 2, 3, and 4 show data from all stations for $O_2/N_2$ ratios, $CO_2$ concentration, and Atmospheric Potential Oxygen (APO, defined below) respectively. Each data point represents averages of two or three replicates collected on the same day. Differences in $O_2/N_2$ ratios are expressed in "per meg" units, where

$$\delta(\mathrm{O_2/N_2})\ \text{(per meg)} = \frac{(\mathrm{O_2/N_2})_{\mathrm{sam}} - (\mathrm{O_2/N_2})_{\mathrm{ref}}}{(\mathrm{O_2/N_2})_{\mathrm{ref}}} \times 10^6, \qquad (1)$$

where $(\mathrm{O_2/N_2})_{\mathrm{sam}}$ is the ratio of the sample gas and $(\mathrm{O_2/N_2})_{\mathrm{ref}}$ is the ratio of an arbitrary reference gas cylinder. 1 per meg is equivalent to 0.001 per mil, the unit typically used in stable isotope work. This ratio is used to define what is meant by $O_2$ concentration. Then by making the assumption that atmospheric $N_2$ concentrations are constant, this definition of $O_2$ concentration can be applied to derive $O_2$ fluxes[1]. In these units, 4.8 per meg are essentially equivalent to 1 ppm (i.e., 1 μmole $O_2$ per mole of dry air). $CO_2$ concentrations are expressed as the mole fraction of dry gas in ppm units. It is also useful (see *Stephens et al.* [1997]) to examine the tracer, Atmospheric Potential Oxygen, which is mostly conservative with respect to $O_2$ and $CO_2$ exchanges in land biota. APO is defined as

$$\text{APO (per meg)} = \delta(\mathrm{O_2/N_2}) + \frac{\alpha_B}{\mathrm{X_{O_2}}}\Delta X_{CO_2}\,, \qquad (2)$$

where $\alpha_B$ represents the $O_2$:$CO_2$ exchange ratio for land biotic photosynthesis and respiration, $\mathrm{X_{O_2}}$ is the standard mole fraction of $O_2$ in dry air, and $\Delta X_{CO_2}$ is the difference in the $CO_2$ mole fraction of the sample from an arbitrary reference gas, in ppm. This definition is a simplified version of the formula presented in *Stephens et al.* [1998] since here we have neglected minor influences from $CH_4$ and CO oxidation. We use $\alpha_B$ = 1.1 based on measurements in *Severinghaus* [1995], and $\mathrm{X_{O_2}}$ = 0.20946 from *Machta and Hughes* [1970]. Variations in APO can only be caused by air-sea exchanges of $O_2$, $N_2$, and $CO_2$, and by combustion of fossil fuels, since the $O_2$:$CO_2$ exchange ratio for fossil fuels is approximately 1.4, different from the value of 1.1 in land biotic exchanges [*Keeling et al.*, 1998b; *Stephens et al.*, 1998].

Since 1989 when our flask sampling program began 5276 flask samples have been collected, of which 5014 have been analysed in our laboratory, and 4653, 4772, and 4644 are presented in the plots of Figures 2, 3, and 4 respectively. Triplicate flasks collected on the same day from the same station are averaged and plotted as a single point in these figures. Reasons for

---

[1] Typical peak $N_2$ fluxes are 6% of $O_2$ fluxes, and because $N_2$ is approximately four times more abundant in the atmosphere, the impact on the atmospheric $O_2/N_2$ ratio is only 1.5% that of $O_2$ fluxes.

non-analysis or exclusion from the plots include flask breakage, identified sampling problems in the field, and procedural problems in our laboratory. For each triplicate, outliers are excluded if they are more than 8 per meg different from the triplicate mean.

All curve fits in Figures 2, 3, and 4, with the exception of Niwot Ridge and Macquarie Island stations, are computed as a least squares fit to the sum of a four harmonic annual seasonal cycle, and a stiff *Reinsch* [1967] spline to account for the interannual trend and other non-seasonal variability. Owing to the shortness of the records, Niwot Ridge and Macquarie Island curve fits are computed as a least squares fit to the sum of a two harmonic annual seasonal cycle and a fixed linear trend.

Several salient features of the data stand out in Figures 2, 3, and 4. All stations exhibit long-term interannual trends, and, with the possible exception of some southern hemisphere stations in $CO_2$, all stations have a clear annual seasonal cycle. Fossil fuel combustion results in the decreasing trend observed in $O_2/N_2$ ratios and APO, and the increasing trend in $CO_2$. Seasonal cycling is predominantly a result of seasonal changes in the growing patterns of biota, predominantly land biota in the case of $CO_2$, marine biota in the case of APO, and a combination of land and marine biota in the case of $O_2/N_2$ ratios. Additional processes can also affect the observed seasonal cycles, in particular other oceanic processes can affect the $O_2/N_2$ ratio and APO cycles, as discussed in the Introduction. Other temporal and spatial features observed in the data are discussed in detail in sections 4 and 5 below.

## 2.3. Data Adjustments

Obtaining $O_2/N_2$ ratio measurements to an accuracy of 5 per meg or better (0.005 ‰) presents many logistical and technical challenges not faced in typical trace gas measurements.

This can be understood conceptually by considering that we are attempting to observe changes in $O_2$ concentrations of 1 part in 209,500. Thus over the years we have continued to discover additional factors and variables in both field sampling methods and instrumental analysis techniques that can create artefacts in $O_2/N_2$ ratios. This section describes those findings only as they pertain to our flask sampling methods, and the subsequent corrections we have applied to the data, where possible.

At Mauna Loa, from inception in January 1991 through to July 1993, $O_2/N_2$ ratio data exhibit greater short-term variability than other stations (see Figure 2). This becomes even more apparent in the Mauna Loa APO plot in Figure 4. At first we reasoned that this scatter in the data could be illustrating real atmospheric variability [*Manning and Keeling*, 1994]. *Heimann et al.* [section 5.5, 1989] have shown that a significant fraction of the $CO_2$ variability observed at Mauna Loa is related to changing synoptic weather patterns particular to the area, further supporting this conclusion. Variations in north-south transport in the proximity of Mauna Loa have the potential to bring air masses of either northern hemisphere or southern hemisphere origin to the area. During much of the year because of both seasonal and anthropogenic effects, these different air masses have large differences in $O_2/N_2$ ratios and $CO_2$ concentrations and this could be reflected by greater variability in $O_2/N_2$ ratios and $CO_2$ concentrations in Mauna Loa flask samples. Indeed, a statistical analysis of these data supported this conclusion, showing that at least 37% of the scatter in the residuals of the flask data from the curve fits could be explained by real atmospheric variability and not by experimental artefacts [*Manning and Keeling*, 1994].

In July 1993, however, it became apparent from communication with Mauna Loa station personnel that the cold trap used to dry the incoming air stream was intermittently leaking. Mauna Loa personnel collect our air samples somewhat differently from all other stations in that the flasks are left flushing overnight for many hours. During this time, ice builds up in the cold trap, causing a slow buildup in the flow restriction and hence increasing the upstream pressure. This pressure could act on the tapered joint seal of the two-piece glass cold trap, periodically breaking the seal and causing intermittent leakage. The positive pressure in the cold trap would probably prevent contamination of room air into the sample, however $O_2$ and $N_2$ would escape from the leak at different rates, fractionating the $O_2/N_2$ ratio of the sample. Once this problem was identified, a new cold trap was sent to Mauna Loa with a different design that would not allow such leakage. Subsequent $O_2/N_2$ ratio and APO data can be seen to exhibit less scatter (Figures 2 and 4). These suspect Mauna Loa data are shown as open circles in Figures 2 and 4, and are not used in subsequent data analyses. Concurrent $CO_2$ data for the same period are also discarded.

In 1998 we discovered that in a flowing air stream $O_2$ will fractionate relative to $N_2$ under many circumstances at a 'tee' junction, where an incoming air stream divides into two outlet air streams [*Manning et al.*, 2002]. Three of our flask sampling stations, Mauna Loa, Samoa, and La Jolla have employed plumbing arrangements with such a tee. At each of these stations the division of flow existed because we shared our intake lines with independent continuous atmospheric $CO_2$ monitoring programs. Recognizing this problem, we set out to eliminate all tees.

At Mauna Loa, the tee was eliminated from the sampling system in June 1998 when we obtained a dedicated intake line. Flask samples were collected simultaneously on the old and new setup at that time and indicated that the tee was producing a –13.5 per meg artifact. This result is further supported by subsequent samples collected, shown in Figures 2 and 4, which appear to indicate a stepwise increase in the data in June 1998 of the order of 10 to 15 per meg (somewhat difficult to see on the low resolution plots presented here). However, based on our experiences of temporal variability in the degree of fractionation at a tee junction [*Manning et al.*, 2002], we can not confidently apply a 13.5 per meg correction to all pre-June 1998 data. Instead, for subsequent data shown and discussed in this paper we have treated Mauna Loa data as two separate time series, with the first terminating in June 1998, and the second beginning at this time. Clearly, the first time series should be considered to contain greater uncertainty than the more recent record.

At Samoa we removed the tee and changed to a dedicated intake line in May 1999. At the same time we shifted the physical location of the intake line from the top of a mast at 42 m a.s.l. to the top of a newly constructed communications tower located approximately 100 m further inland and at a height of 93 m a.s.l. To assess any potential changes in the $O_2/N_2$ ratios or $CO_2$ concentrations of the sampled air created by the removal of the tee or shift in physical location of the inlet, we left the old setup in place and began alternating our biweekly flask collection schedule between the two intakes, starting in May 1999. We continued this for a two year period. A preliminary comparison of the first 12 months of data from this overlapping collection routine shows no discernible difference between the two intakes, although the higher atmospheric variability observed at Samoa, discussed in section 2.4 below, makes a definitive statement difficult.

Flask sampling at La Jolla has undergone a series of transitions. Up until March 1999 sampling took place in a laboratory maintained by C. D. Keeling, approximately 400 meters from the sample intake at the end of the Scripps Pier. Between September 1995 and October 1997, flask samples were also collected from our own laboratories in a different building approximately 100 meters further away from the intake, with different intake tubing and a different pumping module. These samples were collected in addition to and in most cases simultaneously with continued sampling in the C. D. Keeling laboratory. Both of these setups included tees in the intake lines. A comparison of the 32 samples collected simultaneously over this two year period shows a difference of 0.4±3.0 per meg in $O_2/N_2$ ratio, and a difference of 0.03±0.14 ppm in $CO_2$ concentration. These differences are smaller than the laboratory analytical precision. In March 1999, owing to our laboratory moving to a new building, and concerns about the setup in the C. D. Keeling laboratory, we began sampling directly off the end of the Scripps Pier and with no tee. Unfortunately we do not have any overlap of direct pier sampling with either of the old systems, however, a step change such as that observed in the data at Mauna Loa in June 1998 has not been observed at La Jolla.

The question may be asked, why did a tee in the intake line at Mauna Loa cause a –10 to –15 per meg step change in $O_2/N_2$ ratios whereas tees at Samoa and La Jolla appear to have had little or no effect? The answer appears to lie in the flow ratio at the tee junction. The greater the flow ratio of the two outlets of the tee, the greater the potential for $O_2$ fractionation relative to $N_2$ [*Manning et al.*, 2002]. At Mauna Loa, this ratio was typically 15:1.5 Lpm (10), whereas at Samoa and La Jolla it was typically 2:5 Lpm (0.4) and 15:3 Lpm (5) respectively.

$CO_2$ data from Macquarie Island is suspect owing to dry ice being used on site. This problem became apparent from an examination of the residuals of the $CO_2$ flask data points from the curve fit. Macquarie Island residuals exhibited a range of variability greater than ±1.0 ppm, whereas all other mid to high-latitude southern hemisphere stations varied over a range of ±0.5 ppm or less. Therefore subsequent plots and calculations in this paper involving $CO_2$ and APO at Macquarie Island are either not shown, or are calculated by substituting Cape Grim $CO_2$ data as a proxy for this station.

There have been several identified procedural problems with the South Pole sampling program. Several of these have already been discussed in . *Keeling et al.* [1998a]. More recently, we noticed excessive scatter in the 1997 and 1998 data, and in particular we found some flasks to show anomalously high $O_2/N_2$ ratios. We speculate that these values may have been caused during storage after the flask sample had been collected. The flasks were stored in conditions well below freezing. Therefore the stopcock o-rings could have been frozen and it is possible that they did not make a completely leak-tight seal against the glass of the flask. A resultant small leak would produce different leak rates for $O_2$ relative to $N_2$, biasing subsequent measurements of $O_2/N_2$ ratios from the flask. From February 1998 onward, all flask samples were stored in temperatures above freezing, and subsequent data do indeed appear to exhibit less scatter, and furthermore appear to show a change in the long-term trend. Therefore as with Mauna Loa, we have treated the South Pole dataset as two separate time series, before and after February 1998.

Of the six remaining stations in our network, Alert, Cold Bay, Niwot Ridge, Cape Kumukahi, Cape Grim, and Palmer Station, none have ever had a tee in their intake lines, nor have we identified any other significant sampling or procedural problems.

The other potential sources of error or bias in reported flask concentrations are from our laboratory analysis procedures or from long-term drift in our calibration gases. *Keeling et al.* [1998a] give a detailed description of the results from our long-term calibration procedures up to July 1996, and applicable corrections applied to the data. We now have four more years of calibration data and from these no evidence of long term drift in $O_2/N_2$ ratios in our calibration gases is apparent, thus no further corrections have been applied.

For $CO_2$ concentrations our calibration scale has been updated to agree with the Scripps

1999 manometric scale maintained by the C. D. Keeling laboratory, also at Scripps Institution of Oceanography. We also noticed and corrected for a step change in the span of our $CO_2$ analyser in March 1993 which coincided with the change in physical location of our laboratory from Boulder, Colorado, to La Jolla, California. This is perhaps not surprising since in Boulder the $CO_2$ analyser was actively controlled to ambient pressure which is approximately 830 mbar at the altitude of Boulder. When we moved to La Jolla, situated at sea level, we changed the gas handling design so as to continue to actively stabilize the $CO_2$ analyser to 830 mbar. However, it appears that despite our efforts, a change in the span of the analyser occurred. This change was of the order of 0.4 ppm/Volt, which, for example, corresponded to a change in one reference gas of about 0.1 ppm $CO_2$. No changes in $O_2/N_2$ ratios in calibration gases relative to each other were observed after the move to La Jolla.

During a two month period from September to November 1996 a diaphragm on a compressor pump in the analysis system was leaking. This pump is located downstream of the $CO_2$ analyser and so did not affect $CO_2$ concentrations, but, being upstream of the interferometric $O_2$ analyser, it resulted in a change in the $O_2/N_2$ ratio. Because our primary calibration gases were analysed during this period, a correction could be applied to the 136 flasks that were analysed and the data we show in Figures 2 and 4 have this correction applied.

## 3. Global Oceanic and Land Biotic Carbon Sinks

As mentioned in the Introduction, precise measurements of atmospheric $O_2$, along with concurrent $CO_2$ measurements, allow estimates of global oceanic and land biotic carbon sinks to be derived. In this section we present calculations of these sinks made over different time periods and using data from different stations, and we compare our results with results from other researchers.

The primary contribution to the interannual downward trend in $O_2/N_2$ ratios (and upward trend in $CO_2$ concentrations) is anthropogenic combustion of fossil fuels. Other processes can also affect this trend such as biomass burning, anthropogenic land use changes, net uptake by the land biota, and oceanic ventilation processes occurring on interannual time scales. Oceanic uptake of atmospheric $CO_2$, however, reduces the observed upward trend in atmospheric $CO_2$ concentrations, but has no affect on the observed downward trend in $O_2/N_2$ ratios. Thus the global budgets for atmospheric $CO_2$ and $O_2$ can be respectively represented by

$$\Delta CO_2 = F - O - B, \text{ and} \tag{3}$$

$$\Delta O_2 = -\alpha_F F + \alpha_B B + Z, \tag{4}$$

where $\Delta CO_2$ is the globally averaged observed change in atmospheric $CO_2$ concentration, $\Delta O_2$ is the globally averaged observed change in atmospheric $O_2$ concentration, F is the source of $CO_2$ emitted from fossil fuel combustion (and cement manufacture), O is the oceanic $CO_2$ sink, B is the net land biotic $CO_2$ sink (including biomass burning, land use changes, and land biotic uptake), $\alpha_F$ and $\alpha_B$ are the global average $O_2$:$CO_2$ molar exchange ratios for fossil fuels and land biota respectively, and Z is the net exchange of atmospheric $O_2$ with the oceans. All quantities, except for the exchange ratios, $\alpha_F$ and $\alpha_B$, are expressed in units of moles per year.

In all calculations below, a value of $1.10\pm0.05$ is used for $\alpha_B$ [*Severinghaus*, 1995]. That is, 1.1 moles of atmospheric $O_2$ are produced for every mole of atmospheric $CO_2$ consumed by the land biota. An average value of $1.39\pm0.04$ is used for $\alpha_F$ which was calculated from a knowledge of the amount of the different fossil fuel types combusted from year to year [*Marland et al.*, 2002], and from the average $O_2$:C oxidative ratios for full combustion of each fuel type [*Keeling*, 1988a]. This value for $\alpha_F$ was found to change only negligibly for any of the different time periods considered in the sections below (see, for example, Table 3 below).

Previous estimates of global carbon sinks derived from atmospheric $O_2$ and $CO_2$ budgets assumed that there was no oceanic effect on atmospheric $O_2$, that is, the Z term was zero to within the known uncertainties [*Battle et al.*, 2000; *Keeling et al.*, 1996; *Keeling and Shertz*, 1992]. In terms of exchange owing to the atmosphere-ocean equilibrium shift caused by decreasing atmospheric $O_2$ driven by fossil fuel combustion, this assumption holds well, because $O_2$ is much less soluble in seawater than $CO_2$. However, there is another process that can cause significant net air-sea gas exchange and that is net ocean warming (or cooling). Recently, *Levitus et al.* [2000] showed that the global oceans have warmed significantly since 1948. For example, they calculated that the temperature of the 0 to 300 meter layer of the global ocean increased by 0.31°C over 40 years. Such warming can result in oceanic $O_2$ outgassing due to changes in both the solubility and biological pumps, as discussed by Sarmiento *et al.* [1998], and will offset the observed atmospheric $O_2$ decrease. Recently, attempts have been made to quantify the amount of oceanic $O_2$ outgassed during different periods over the last couple of decades, using both ocean general circulation models [*Bopp et al.*, 2001; *Plattner et al.*, 2002], and using observational data of dissolved $O_2$ and phosphate concentrations and climatological air-sea heat fluxes [*Keeling and Garcia*, 2002].

Previously, to solve for the oceanic and land biotic carbon sinks Equation 4 above has been used to obtain the land biotic sink and then Equation 3 has been applied to obtain the oceanic sink ([*Keeling et al.*, 1996; *Keeling and Shertz*, 1992]). Here we use a different methodology. We combine Equations 2, 3 and 4 to give

$$\Delta APO = (-\alpha_F + \alpha_B)F - \alpha_B O + Z \tag{5}$$

where ΔAPO is the globally averaged observed change in Atmospheric Potential Oxygen. We use Equation 5 to obtain the oceanic sink and then use Equation 3 to obtain the land biotic sink. There are several reasons for using this methodology.

First, in deriving the oceanic sink, the uncertainty calculated from a quadrature sum of errors is reduced by using Equation 5. Second, uncertainty is further reduced because short-term (daily to seasonal) atmospheric variability is less in APO than in $O_2/N_2$ ratios. Third, we expect longer term interannual variability in APO to be reduced compared to $O_2/N_2$ ratios because the APO signal is not affected by interannual variability in the land biotic sink, and indeed APO data shown in Figure 6 appear to confirm this, exhibiting less variability than comparative $O_2/N_2$ ratio data in Figure 5 (These two figures are discussed in Section 4 below). Once we have obtained the oceanic sink from Equation 5, we then have the choice of using either Equation 3 or 4 to derive the land biotic sink. We chose to use Equation 3, both because it avoids applying the oceanic $O_2$ outgassing term a second time, a parameter which is known only very poorly, and because with Equation 3 we have the option of using global atmospheric $CO_2$ datasets from other sources to derive $\Delta CO_2$, in particular the NOAA/CMDL global network, which has a much denser global coverage than our own network, thus giving a more robust estimate of the land biotic sink.

Several simplifying assumptions have been applied in formulating Equations 3, 4, and 5. We assume that there is no longterm net change in marine productivity (which would affect atmospheric $O_2$); we assume no longterm (interannual) oceanic $O_2$ ventilation other than that associated with oceanic warming effects, accounted for in our Z term; we have included a Z term for $N_2$ as a correction factor to the observed atmospheric $O_2/N_2$ ratio, but we only calculate oceanic $N_2$ outgassing caused directly by changes in solubility resulting from ocean warming; we assume that there is no Z term for $CO_2$; and in Equation 5, we assume that the $O_2$:$CO_2$ molar exchange ratio of all land biota (that is, $\alpha_B$) is 1.10, and that influences on APO due to oxidation of $CH_4$ and CO are negligible.

## 3.1. Calculation for the Decade of the 1990s

The data and results presented in this section have been used in the IPCC (Intergovernmental Panel for Climate Change) Third Assessment Report ([*Prentice et al.*, 2001]), in their presentation of the oceanic and land biotic sinks for the decade of the 1990s. The IPCC referenced Manning [2001]. However, Manning [2001] is a Ph.D. dissertation, and thus is not a formally published or peer-reviewed document. For this reason, and because of the interest shown by many workers, the work of Manning [2001] is duplicated here. Furthermore, we provide detailed tables of data so that our calculations can be repeated by other researchers if desired.

We calculate global averages of APO and $CO_2$ by using data from selected stations in our global network. For each station used we use the curve fits to the flask data shown in Figures 3 and 4 to adjust all flask data to the 15th of each month, then we calculate monthly means. Months with no flask data are filled in using the curve fits. We average twelve consecutive monthly means to compute annual means for APO and $CO_2$, repeating this calculation at six-month time steps centered on 1 January and 1 July of each year. The IPCC wished to report global oceanic and land biotic carbon sinks for the entire decade of the 1990s so as to compare these results with similar results computed for the 1980s decade. Eleven years of APO and $CO_2$ data are needed in order to perform these calculations for the ten year period from 1 January 1990 to 1 January 2000. The technique subtracts an annual average centered on 1 January 2000 from an annual average centered on 1 January 1990, and therefore requires atmospheric measurements spanning the period from 1 July 1989 to 1 July 2000. La Jolla is the only station for which such a dataset exists. The Alert record comes close, with samples collected on two dates in 1989, in November and December. Therefore our strategy is to use both the La Jolla and Alert records, with a slightly different method of calculating the beginning point of the Alert record.

In the Appendix we assess the robustness of the Alert beginning point calculation, comment on not using any data from a southern hemisphere station, and detail other considerations that were necessary to arrive at these particular results. Table 2 shows annual averages of $O_2/N_2$ ratio data and calculated APO data for La Jolla, Alert, and the average of these two stations. These APO annual averages are shown graphically as solid circles in Figure 7, which shows also calculated annual averages of $CO_2$. These data points show the expected trends of decreasing APO over time and increasing $CO_2$ concentrations.

We calculate the amount of $CO_2$ produced from fossil fuel combustion and cement manufacture from data in *Marland et al.* [2002]. We calculate the amount of $O_2$ (and thus APO) consumed from a knowledge of the relative fraction of the different fossil fuel types combusted each year and the $O_2$:$CO_2$ oxidative ratios for each fuel type given in *Keeling* [1988a], assuming full combustion of fossil fuel carbon to $CO_2$. These data are shown in Table 3. For the ten year period from January 1990 to January 2000 these fossil fuel emissions resulted in 63.3±3.8 Gt C of $CO_2$ being released to the atmosphere (F in Equations 3, 4, and 5; see also penultimate row of Table 3), and, if no other processes were involved, would have resulted in a total APO decrease of 41.8±2.5 per meg and an atmospheric $CO_2$ increase of 29.8±1.8 ppm. These hypothetical APO and $CO_2$ changes are shown in Figure 7 as a straight line labelled "change due to fossil fuel combustion only". However, the observed atmospheric changes over this ten year period were an APO decrease of 81.7±6.0 per meg (ΔAPO in Equation 5), and an atmospheric $CO_2$ increase of 15.11±0.61 ppm (32.1±1.3 Gt C; $\Delta CO_2$ in Equation 3). The value for ΔAPO was found simply by subtracting the 1990.0 mean from the 2000.0 mean (see Table 2). For $\Delta CO_2$, however, as proposed above, we have used NOAA/CMDL data [*Conway et al.*, 1994]. In this particular calculation, this has the additional advantage of allowing us to include southern hemisphere stations in the global average for $\Delta CO_2$ since the NOAA dataset includes such stations extending back in time to at least 1990. Thus the global value for $\Delta CO_2$ was determined (P. Tans, personal communication) using a 2-D atmospheric transport model described in *Tans et al.* [*Tans et al.*, 1989].

Setting the Z term (Equation 5) to zero for the moment, it is a useful exercise to calculate average oceanic and land biotic sinks assuming no oceanic $O_2$ outgassing term. From the data above this results in:

oceanic carbon sink = 1.62±0.50 Gt C/y, and
land biotic carbon sink = 1.51±0.64 Gt C/y.

These results are illustrated graphically in Figure 7.

As mentioned above, the oceanic $O_2$ outgassing term, Z, should incorporate effects due to both the solubility and biological pumps. Three recent studies [*Bopp et al.*, 2001; *Keeling and Garcia*, 2002; *Plattner et al.*, 2002] have produced estimates for Z, however, at the time the IPCC report was published none of these studies had been completed. Therefore, in faithfulness to our duplication of our work for the IPCC, we derive here our own estimate for the solubility-only effect on oceanic $O_2$ outgassing. Because the effects of ocean warming on the biological pump are more complex and poorly understood, we make no attempt here to correct for any possible effects.

We assume a 1 W/m$^2$ warming rate over the global oceans during the 1990s (M. Heimann, personal communication). This corresponds to a 0.71 W/m$^2$ warming over the entire surface of the Earth. Because of the uncertain nature of this calculation, we assign a 100% uncertainty to this warming rate. 1 W/m$^2$ results in a total of 1.14 x 10$^{23}$ J of energy being absorbed by the oceans during the decade of the 1990s. Using an $O_2$ solubility temperature dependence of 5.818 x 10$^{-6}$ mol/kg/K [*Weiss*, 1970], this results in a total of 1.59 x 10$^{14}$ mol $O_2$ outgassed from the oceans in the 1990s. Net $N_2$ outgassing from the oceans will also occur, offsetting the increase in the atmospheric $O_2/N_2$ ratio. We calculate that 2.58 x 10$^{14}$ mol $N_2$ outgassed from the oceans in the 1990s, or 0.69 x 10$^{14}$ mol $O_2$ equivalent. Therefore 0.90 x 10$^{14}$ mol $O_2$ were effectively outgassed after applying this $N_2$ correction. Recalculating the average oceanic and land biotic carbon sinks in the 1990s results in:

oceanic carbon sink = 1.71±0.52 Gt C/y, and
land biotic carbon sink = 1.41±0.66 Gt C/y. [1]

These results show that the global oceanic and land biotic carbon sinks are of approximately comparable magnitude and importance in the global carbon budget. These results also show an approximate 0.1 Gt C/y shift in both sinks when allowance is made for an ocean warming effect with subsequent $O_2$ outgassing caused by solubility pump changes, with the oceanic sink becoming larger and the land biotic sink smaller. It is important to keep in mind with these IPCC results that additional oceanic $O_2$ outgassing most probably occurred owing to

---

[1] There are two minor differences in the calculation presented here compared to that of Manning [, 2001 #725]. First, Manning [, 2001 #725] did not have available fossil fuel emission data from Marland *et al.* [, 2002 #653] through to the end of 1999, instead using data from British Petroleum for emissions in 1998 and 1999 (H. Kheshgi, personal communication). Second, at that time the Alert record went only as far as May 2000, two months short of the July 2000 required to achieve an annual average centred on 1 January 2000. Therefore a slightly different technique was used to obtain this year 2000 annual average. The resulting differences between the oceanic and land biotic sinks of Manning [, 2001 #725] and those presented here was only 0.03 Pg C/y. Therefore to a precision of one decimal place, as presented in the IPCC report, the results are the same.

biological pump changes induced by the ocean warming trend, and that this would result in a larger oceanic carbon sink and a smaller land biotic carbon sink than calculated here.

We would also like to make it explicitly clear that this calculation technique effectively determines a global oceanic carbon sink from northern hemisphere data only, then using this oceanic sink result, the land biotic sink is calculated from globally averaged $CO_2$ data. This provides a more robust estimate of the land biotic sink, advantageous since the land sink exhibits much greater natural variability than the oceanic sink (see section 3.4 below). In addition, the land biotic sink can be expected to show greater north-south asymmetry than the oceanic sink, thus greater bias would result if the land biotic sink was also calculated from northern hemisphere-only data.

## 7. Appendix:

### Additional Considerations for the 1990s Global Sinks Calculation

In this section we give further details on additional considerations that were necessary to arrive at the global sink calculations presented in section 3.1. We also detail how we arrived at the uncertainties given for these sinks. In the La Jolla dataset we discarded some data from flask samples collected in 1990. This is pertinent to any comparison made to *Keeling and Shertz* [1992], where our 1990 data were also used. In 1989 and 1990, some of the stopcocks on the glass flasks sealed with Teflon o-rings, rather than Viton o-rings. *Keeling and Shertz* [1992], observing very low $O_2$ concentrations in some flask samples, realized that they were contaminated, and attributed this problem to preferential diffusion of $O_2$ relative to $N_2$ through the Teflon o-rings. *Keeling and Shertz* [1992] discarded many, but not all, of the samples collected in these flasks. With the longer dataset now available, we were able to show that the Teflon o-ring-sealed flasks retained by *Keeling and Shertz* [1992] also exhibited a small negative $O_2$ anomaly from the apparent baseline. Therefore we discarded all remaining samples collected in Teflon o-ring-sealed flasks. Although $CO_2$ concentrations were not affected by the Teflon o-ring-sealed flasks, we removed $CO_2$ data obtained from the same flasks also, so as not to cause inconsistent aliasing of the two datasets. This removed seven sampling dates in 1990 from the dataset, leaving a total of five dates when samples were collected from La Jolla in 1989 and three in 1990 (in 1991 our regular sampling program was initiated and, for example, in this year 18 samples were collected). The raw data retained are shown in Figure 8a. Here we have shown APO data only, and we have seasonally detrended the data, removing the four-harmonic component of the curve fit from all data points. Therefore this figure shows the actual data used to compute the annual means.

Because of the sparseness of the early part of the La Jolla record, we then proceeded to look in more detail at the Alert record. If the Alert record shows a similar long-term trend as La Jolla, then this will provide greater confidence in the La Jolla data. Flask samples were collected on two dates at Alert in 1989, none in 1990, and 15 in 1991 when a regular sampling program was begun. Figure 8b shows the Alert seasonally detrended APO.

In order to include the Alert data in the oceanic and land biotic sink calculations, annual averages centered on 1 January 1990, and 1 January 2000 are needed, therefore requiring data back to 1 July 1989, and up to 1 July 2000 in the normal calculation methods. Since in 1989 we only have data from samples collected in November and December, our procedure to calculate an “annual” average was as follows: The computer program used for calculating curve fits to the data also reports monthly values of the curve fit on the 15th of each month, and reports deseasonalized values for each month. Therefore we averaged four deseasonalized monthly values, from November and December 1989, based on flask samples, and from January and February 1990, based on interpolated monthly values of the curve fit, resulting in an average centered on 1 January 1990.

The advantages of using APO data instead of $O_2/N_2$ ratio data have been mentioned in Section 3 above. For the unique case of these IPCC calculations, using APO is even more advantageous, helping reduce additional uncertainty that could have arisen both due to the sparseness of the early La Jolla and Alert records, and the necessary interpolation of the early Alert record. This becomes apparent when we compare longterm trends at La Jolla and Alert in $O_2/N_2$ ratios and APO over different time periods. For the nine year period starting in 1991 when sampling programs were in full operation at both stations, the $O_2/N_2$ ratio trend differed by about 5 per meg over the nine years. Whereas with the interpolated Alert dataset, and the sparse early record of La Jolla added, the difference in the trends doubles to 10 per meg over ten years. However, APO data over the same intervals (illustrated in Figure 8) show only a 2 per meg difference in the Alert and La Jolla trends over nine years, and also a 2 per meg difference over the longer ten year period. These findings provide confidence both in the use of APO data, and in the Alert interpolation technique and subsequent averaging of Alert and La Jolla stations to obtain a northern hemisphere proxy.

The final consideration in the IPCC calculation is the lack of southern hemisphere $O_2/N_2$ data in computing “global” carbon sinks. Not only is there an interhemispheric gradient in $O_2/N_2$ ratios and APO [*Stephens et al.*, 1998], but these gradients exhibit significant interannual variability. This makes it problematic to use only northern hemisphere stations in calculating a global average. We attempted to quantify this additional error by comparing the Cape Grim trend to the Alert and La Jolla trends over the time period for which we have Cape Grim data, which is a 9.5 year measurement period from January 1991 to July 2000. Over this time period, the $O_2/N_2$ ratio at Cape Grim decreased by about 15 per meg more than at the two northern hemisphere stations. In APO the difference was less, but still high at about 10 per meg. Since in a true global calculation the southern hemisphere would contribute a weighting of one-half to the global trend, we decided to add ±3 per meg uncertainty to the reported APO trend because of this lack of southern hemisphere data.

A summary of the uncertainties assigned to the different variables used in the global sinks calculation is shown in Table 4. The total uncertainty in the assigned global APO trend is ±8.2 per meg. This was derived from a quadrature sum of the ±6 per meg uncertainty for a typical global $O_2/N_2$ (or APO) trend computation [*Keeling et al.*, 1996], ±3 per meg attributed to the lack of southern hemisphere data, ±3.4 per meg additional uncertainty attributed to sparse data in the early Alert record and the Alert interpolation, and ±3.2 per meg attributed to the sparse La Jolla data in 1989 and 1990. These latter two uncertainties were calculated by considering the residuals of the flask data from the curve fits of the full Alert and La Jolla records. These residuals are shown in Figure 9. The standard deviation of these residuals was calculated for the full record, then the standard error was calculated by considering how many flask samples were used in deriving the 1990 annual averages. Figure 9 also aids in verifying that the 1989 and 1990 data are not unusual in terms of their residuals from the fitted curves.

## 8. References

Bacastow, R.B., C.D. Keeling, T.J. Lueker, M. Wahlen, and W.G. Mook, The $^{13}C$ Suess effect in the world surface oceans and its implications for oceanic uptake of $CO_2$: Analysis of observations at Bermuda, *Global Biogeochemical Cycles*, *10* (2), 335-346, 1996.

Balkanski, Y., P. Monfray, M. Battle, and M. Heimann, Ocean primary production derived from satellite data: An evaluation with atmospheric oxygen measurements, *Global Biogeochemical Cycles*, *13* (2), 257-271, 1999.

Battle, M., M. Bender, T. Sowers, P.P. Tans, J.H. Butler, J.W. Elkins, J.T. Ellis, T. Conway, N. Zhang, P. Lang, and A.D. Clarke, Atmospheric gas concentrations over the past century measured in air from firn at the South Pole, *Nature*, *383*, 231-235, 1996.

Battle, M., M.L. Bender, P.P. Tans, J.W.C. White, J.T. Ellis, T. Conway, and R.J. Francey, Global carbon sinks and their variability inferred from atmospheric $O_2$ and $\delta^{13}C$, *Science*, *287* (5462), 2467-2470, 2000.

Bender, M., T. Ellis, P. Tans, R. Francey, and D. Lowe, Variability in the $O_2/N_2$ ratio of southern hemisphere air, 1991-1994: Implications for the carbon cycle, *Global Biogeochemical Cycles*, *10* (1), 9-21, 1996.

Bender, M.L., M. Battle, and R.F. Keeling, The $O_2$ balance of the atmosphere: A tool for studying the fate of fossil-fuel $CO_2$, *Annu. Rev. Energy Environ.*, *23*, 207-223, 1998.

Bender, M.L., and M.O. Battle, Carbon cycle studies based on the distribution of $O_2$ in air, *Tellus Series B-Chemical and Physical Meteorology*, *51* (2), 165-169, 1999.

Bender, M.L., T. Sowers, J.M. Barnola, and J. Chappellaz, Changes in the $O_2/N_2$ ratio of the atmosphere during recent decades reflected in the composition of air in the firn at Vostok Station, Antarctica, *Geophysical Research Letters*, *21*, 189-192, 1994a.

Bender, M.L., P.P. Tans, J.T. Ellis, J. Orchardo, and K. Habfast, A high precision isotope ratio mass spectrometry method for measuring the $O_2/N_2$ ratio of air, *Geochimica et Cosmochimica Acta*, *58* (21), 4751-4758, 1994b.

Benedict, F.G., *The Composition of the Atmosphere with Special Reference to its Oxygen Content*, Carnegie Institution of Washington, 1912.

Bloom, A.J., R.M. Caldwell, J. Finazzo, R.L. Warner, and J. Weissbart, Oxygen and carbon dioxide fluxes from barley shoots depend on nitrate assimilation, *Plant Physiology*, *91* (1), 352-356, 1989.

Bopp, L., C. Le Quere, M. Heimann, A.C. Manning, and P. Monfray, Climate-induced oceanic oxygen fluxes: Implications for the contemporary carbon budget, GBC, 2001.

Carpenter, T.M., The constancy of the atmosphere with respect to carbon dioxide and oxygen content, *J. Amer. Chem. Soc.*, *59*, 358-360, 1937.

Ciais, P., P.P. Tans, J.W.C. White, M. Trolier, R.J. Francey, J.A. Berry, D.R. Randall, P.J. Sellers, J.G. Collatz, and D.S. Schimel, Partitioning of ocean and land uptake of $CO_2$ as inferred by $\delta^{13}C$ measurements from the NOAA Climate Monitoring and Diagnostics Laboratory Global Air Sampling Network, *Journal of Geophysical Research*, *100* (D3), 5051-5070, 1995.

Conway, T.J., P.P. Tans, L.S. Waterman, K.W. Thoning, D.R. Kitzis, K.A. Masarie, and N. Zhang, Evidence for interannual variability of the carbon cycle from the NOAA/CMDL global air sampling network, *Journal of Geophysical Research*, *99* (D11), 22,831-22,855, 1994.

Enting, I.G., C.M. Trudinger, and R.J. Francey, A synthesis inversion of the concentration and $\delta^{13}C$ of atmospheric $CO_2$, *Tellus Series B-Chemical and Physical Meteorology*, *47* (1-2), 35-52, 1995.

GLOBALVIEW-CO2, GLOBALVIEW-CO2: Cooperative Atmospheric Data Integration Project - Carbon Dioxide, CD-ROM, NOAA/CMDL, Boulder, Colorado. [Also available on Internet via anonymous FTP to ftp.cmdl.noaa.gov, Path: ccg/co2/GLOBALVIEW], 1999.

Graedel, T.E., and P.J. Crutzen, *Atmospheric change: an Earth system perspective*, 446 pp., W. H. Freeman and Company, New York, 1993.

Gruber, N., and C.D. Keeling, The isotopic air-sea disequilibrium and the oceanic uptake of anthropogenic $CO_2$, in *Proceedings of the 2nd International Symposium, $CO_2$ in the Oceans*, Center for Global Environmental Research, National Institute for Environmental Studies, Tsukuba, Japan, 1999.

Heimann, M., C.D. Keeling, and C.J. Tucker, A three-dimensional model of atmospheric $CO_2$ transport based on observed winds: 3. Seasonal cycle and synoptic time scale variations, in *Geophysical Monograph 55, Aspects of climate variability in the Pacific and the Western Americas*, edited by D.H. Peterson, pp. 277-303, American Geophysical Union, Washington D. C., 1989.

Heimann, M., and E. Maier-Reimer, On the relations between the oceanic uptake of $CO_2$ and its carbon isotopes, *Global Biogeochemical Cycles*, *10* (1), 89-110, 1996.

Keeling, C.D., S.C. Piper, and M. Heimann, A three-dimensional model of atmospheric $CO_2$ transport based on observed winds: 4. Mean annual gradients and interannual variations, in *Geophysical Monograph 55, Aspects of climate variability in the Pacific and the Western Americas*, edited by D.H. Peterson, pp. 305-363, American Geophysical Union, Washington D. C., 1989.

Keeling, R.F., Development of an interferometric oxygen analyzer for precise measurement of the atmospheric $O_2$ mole fraction, Ph.D. thesis, Harvard University, Cambridge, Massachusetts, U.S.A., 1988a.

Keeling, R.F., Measuring correlations between atmospheric oxygen and carbon dioxide mole fractions: A preliminary study in urban air, *Journal of Atmospheric Chemistry*, *7*, 153-176, 1988b.

Keeling, R.F., and H.E. Garcia, The change in oceanic $O_2$ inventory associated with recent global warming, *Proceedings of the National Academy of Sciences of the United States of America*, *99* (12), 7848-7853, 2002.

Keeling, R.F., A.C. Manning, E.M. McEvoy, and S.R. Shertz, Methods for measuring changes in atmospheric $O_2$ concentration and their applications in southern hemisphere air, *Journal of Geophysical Research*, *103* (D3), 3381-3397, 1998a.

Keeling, R.F., R.P. Najjar, M.L. Bender, and P.P. Tans, What atmospheric oxygen measurements can tell us about the global carbon cycle, *Global Biogeochemical Cycles*, *7* (1), 37-67, 1993.

Keeling, R.F., S.C. Piper, and M. Heimann, Global and hemispheric $CO_2$ sinks deduced from changes in atmospheric $O_2$ concentration, *Nature*, *381*, 218-221, 1996.

Keeling, R.F., and S.R. Shertz, Seasonal and interannual variations in atmospheric oxygen and implications for the global carbon cycle, *Nature*, *358*, 723-727, 1992.

Keeling, R.F., B.B. Stephens, R.G. Najjar, S.C. Doney, D. Archer, and M. Heimann, Seasonal variations in the atmospheric $O_2/N_2$ ratio in relation to the kinetics of air-sea gas exchange, *Global Biogeochemical Cycles*, *12* (1), 141-163, 1998b.

Langenfelds, R.L., R.J. Francey, L.P. Steele, M. Battle, R.F. Keeling, and W.F. Budd, Partitioning of the global fossil $CO_2$ sink using a 19-year trend in atmospheric $O_2$, *Geophysical Research Letters*, *26* (13), 1897-1900, 1999.

Levitus, S., J.I. Antonov, T.P. Boyer, and C. Stephens, Warming of the world ocean, *Science*, *287* (5461), 2225-2229, 2000.

Liss, P.S., and L. Merlivat, Air-sea gas exchange rates: Introduction and synthesis, in *The Role of Air-Sea Exchange in Geochemical Cycling*, edited by P. Buat-Menard, pp. 113-127, D Reidel, Norwell, Mass, 1986.

Machta, L., Oxygen depletion, in *Proceedings of the International Meeting on Stable Isotopes in Tree Ring Research*, edited by G.C. Jacoby, pp. 125-127, 1980.

Machta, L., and E. Hughes, Atmospheric oxygen in 1967 to 1970, *Science*, *168*, 1582-1584, 1970.

Mann, M.E., R.S. Bradley, and M.K. Hughes, Global-scale temperature patterns and climate forcing over the past six centuries, *Nature*, *392* (6678), 779-787, 1998.

Manning, A.C., Temporal variability of atmospheric oxygen from both continuous measurements and a flask sampling network: Tools for studying the global carbon cycle, Ph. D. thesis, University of California, San Diego, La Jolla, California, U.S.A., 2001.

Manning, A.C., and R.F. Keeling, Correlations in short-term variations in atmospheric oxygen and carbon dioxide at Mauna Loa Observatory, in *Climate Monitoring and Diagnostics Laboratory, No. 22, Summary Report 1993*, edited by J.T. Peterson, and R.M. Rosson, pp. 121-123, U.S. Department of Commerce, NOAA Environmental Research Laboratories, Boulder, CO, 1994.

Manning, A.C., R.F. Keeling, and J.P. Severinghaus, Precise atmospheric oxygen measurements with a paramagnetic oxygen analyzer, *Global Biogeochemical Cycles*, *13* (4), 1107-1115, 1999.

Manning, A.C., M.R. Manning, G.W. Brailsford, A.J. Gomez, R.F. Keeling, W.J. Paplawsky, and C.G. Atwood, Oceanic and terrestrial contributions to atmospheric $O_2$ and $CO_2$ derived from continuous measurements at Baring Head, New Zealand, 2002.

Marland, G., T.A. Boden, and R.J. Andres, Global, Regional, and National Annual CO2 Emissions from Fossil-Fuel Burning, Cement Production, and Gas Flaring: 1751-1999, Carbon Dioxide Information Analysis Center, Oak Ridge National Laboratory, U.S. Department of Energy, Oak Ridge, Tenn., U.S.A., 2002.

Orr, J.C., *Ocean Carbon-Cycle Model Intercomparison Project (OCMIP)*, 27 pp., 1997.

Peixoto, J.P., and A.H. Oort, *Physics of climate*, 520 pp., American Institute of Physics, New York, 1992.

Plattner, G.K., F. Joos, and T.F. Stocker, Revision of the global carbon budget due to changing air-sea oxygen fluxes, GBC, 2002.

Prentice, I.C., G.D. Farquhar, M.J.R. Fasham, M.L. Goulden, M. Heimann, V.J. Jaramillo, H.S. Kheshgi, C. Le Quéré, R.J. Scholes, and D.W.R. Wallace, The Carbon Cycle and Atmospheric $CO_2$, in *Climate Change 2001: The Scientific Basis.*

*Contribution of Working Group I to the Third Assessment Report of the Intergovernmental Panel on Climate Change (IPCC)*, edited by J.T. Houghton, Y. Ding, D.J. Griggs, M. Noguer, P.J. van der Linden, and D. Xiaosu, pp. 944, Cambridge University Press, Cambridge, 2001.

Quay, P.D., B. Tilbrook, and C.S. Wong, Oceanic uptake of fossil fuel $CO_2$: Carbon-13 evidence, *Science*, *256*, 74-79, 1992.

Reinsch, C.M., Smoothing by spline functions, *Num. Math.*, *10*, 177-183, 1967.

Sarmiento, J.L., T.M.C. Hughes, R.J. Stouffer, and S. Manabe, Simulated response of the ocean carbon cycle to anthropogenic climate warming, *Nature*, *393*, 245-249, 1998.

Severinghaus, J.P., Studies of the terrestrial $O_2$ and carbon cycles in sand dune gases and in Biosphere 2, Ph.D. thesis, Columbia University, New York, U.S.A., 1995.

Stephens, B.B., Field-based atmospheric oxygen measurements and the ocean carbon cycle, Ph. D. thesis, University of California, San Diego, La Jolla, California, U.S.A., 1999.

Stephens, B.B., R.F. Keeling, M. Heimann, K.D. Six, R. Murnane, and K. Caldeira, Testing global ocean carbon cycle models using measurements of atmospheric $O_2$ and $CO_2$ concentration, in *Global Biogeochemical Cycles*, 1997.

Stephens, B.B., R.F. Keeling, M. Heimann, K.D. Six, R. Murnane, and K. Caldeira, Testing global ocean carbon cycle models using measurements of atmospheric $O_2$ and $CO_2$ concentration, *Global Biogeochemical Cycles*, *12* (2), 213-230, 1998.

Takahashi, T., R.H. Wanninkhof, R.A. Feely, R.F. Weiss, D.W. Chipman, N. Bates, J. Olafsson, C. Sabine, and S.C. Sutherland, Net sea-air $CO_2$ flux over the global oceans: an improved estimate based on the sea-air $CO_2$ difference, in *Proceedings of the 2nd International Symposium, $CO_2$ in the Oceans*, pp. 9-14, Center for Global Environmental Research, National Institute for Environmental Studies, Tsukuba, Japan, 1999.

Tans, P.P., P.S. Bakwin, and D.W. Guenther, A feasible global carbon cycle observing system: A plan to decipher today's carbon cycle based on observations, *Global Change Biology*, *2*, 309-318, 1996.

Tans, P.P., J.A. Berry, and R.F. Keeling, Oceanic $^{13}C/^{12}C$ observations: a new window on ocean $CO_2$ uptake, *Global Biogeochemical Cycles*, *7* (2), 353-368, 1993.

Tans, P.P., T.J. Conway, and T. Nakazawa, Latitudinal distribution of the sources and sinks of atmospheric carbon dioxide derived from surface observations and an atmospheric transport model, *Journal of Geophysical Research*, *94* (D4), 5151-5172, 1989.

Tans, P.P., I.Y. Fung, and T. Takahashi, Observational constraints on the global atmospheric $CO_2$ budget, *Science*, *247*, 1431-1438, 1990.

Tohjima, Y., Method for measuring changes in the atmospheric $O_2/N_2$ ratio by a gas chromatograph equipped with a thermal conductivity detector, *Journal of Geophysical*

*Research-Atmospheres*, *105* (D11), 14575-14584, 2000.

Weiss, R.F., The solubility of nitrogen, oxygen and argon in water and seawater, *Deep-Sea Research*, *17*, 721-735, 1970.

-

**Table 1.** Flask Sampling Stations in the Scripps $O_2/N_2$ Network

| Station code | Station | Latitude | Longitude | Elevation (m a.s.l.) | Time period |
|---|---|---|---|---|---|
| ALT | Alert, Northwest Territories, Canada | 82°27'N | 62°31'W | 210 | Nov. 1989 – May 2000 |
| CBA | Cold Bay, Alaska, USA | 55°12'N | 162°43'W | 25 | Aug. 1995 – May 2000 |
| NWR | Niwot Ridge, Colorado, USA | 40°03'N | 105°38'W | 3749 | Apr. 1991 – Apr. 1993 |
| LJO | La Jolla, California, USA | 32°52'N | 117°15'W | 15 | May 1989 – June 2000 |
| MLO | Mauna Loa, Hawaii, USA | 19°32'N | 155°35'W | 3397 | Jan. 1991 – May 2000 |
| KUM | Cape Kumukahi, Hawaii, USA | 19°31'N | 154°49'W | 3 | June 1993 – May 2000 |
| SMO | Cape Matatula, American Samoa, USA | 14°15'S | 170°34'W | 42/93[*] | June 1993 – Apr. 2000 |
| CGO | Cape Grim, Tasmania, Australia | 40°41'S | 144°41'E | 94 | Jan. 1991 – Dec. 1999 |
| MCQ | Macquarie Island, Australia | 54°29'S | 158°58'E | 94 | Sep. 1992 – Jan. 1994 |
| PSA | Palmer Station, Antarctica | 64°55'S | 64°00'W | 10 | Sep. 1996 – Mar. 2000 |
| SPO | South Pole Station, Antarctica | 89°59'S | 24°48'W | 2810 | Nov. 1991 – Dec 1999 |

[*] In May 1999 a new sampling intake was installed on a new tower, 93 m above sea level.

**Table 2.** Globally and Annually Averaged Trends in the 1990s[1]

| | $O_2/N_2$ (per meg) | | | APO[2] (per meg) | | |
|---|---|---|---|---|---|---|
| Year | Alert | La Jolla | Average | Alert | La Jolla | Average |
| 1990.0 | -111.1 | -95.7 | -103.4 | -75.6 | -74.7 | -75.1 |
| 1990.5 | -117.7 | -107.3 | -112.5 | -81.5 | -79.9 | -80.7 |
| 1991.0 | -123.3 | -113.8 | -118.6 | -87.2 | -83.5 | -85.4 |
| 1991.5 | -131.4 | -125.1 | -128.2 | -93.2 | -89.3 | -91.3 |
| 1992.0 | -140.8 | -127.9 | -134.4 | -100.2 | -90.7 | -95.4 |
| 1992.5 | -141.6 | -129.0 | -135.3 | -102.6 | -94.1 | -98.3 |
| 1993.0 | -142.1 | -134.7 | -138.4 | -103.3 | -98.9 | -101.1 |
| 1993.5 | -149.3 | -140.6 | -144.9 | -109.0 | -101.6 | -105.3 |
| 1994.0 | -158.4 | -150.4 | -154.4 | -113.6 | -106.5 | -110.1 |
| 1994.5 | -168.3 | -162.4 | -165.3 | -117.2 | -110.1 | -113.7 |
| 1995.0 | -180.2 | -169.3 | -174.8 | -125.3 | -112.5 | -118.9 |
| 1995.5 | -191.5 | -178.5 | -185.0 | -131.2 | -115.7 | -123.4 |
| 1996.0 | -197.0 | -192.3 | -194.6 | -130.9 | -123.8 | -127.4 |
| 1996.5 | -204.7 | -196.9 | -200.8 | -132.9 | -129.8 | -131.3 |
| 1997.0 | -211.2 | -201.8 | -206.5 | -136.7 | -132.9 | -134.8 |
| 1997.5 | -216.1 | -209.9 | -213.0 | -139.1 | -136.1 | -137.6 |
| 1998.0 | -225.4 | -217.8 | -221.6 | -143.4 | -139.1 | -141.2 |
| 1998.5 | -236.2 | -229.4 | -232.8 | -146.7 | -143.0 | -144.9 |
| 1999.0 | -244.6 | -239.9 | -242.2 | -147.1 | -145.1 | -146.1 |
| 1999.5 | -250.8 | -245.3 | -248.0 | -150.8 | -147.2 | -149.0 |
| 2000.0 | -260.4 | -255.7 | -258.1 | -157.0 | -154.4 | -155.7 |
| Trend[3] | -149.4 | -160.0 | -154.7 | -81.43 | -79.73 | -80.58 |
| Trend ($10^{14}$ mol)[4] | -55.36 | -59.31 | -57.34 | -30.18 | -29.55 | -29.87 |

[1] All data are annual averages, calculated every six months, centered on 1 January and 1 July of each year, as described in the text (section 3.1). The average columns are the average of Alert and La Jolla.

[2] APO, Atmospheric Potential Oxygen, is defined in section 2.2, and is essentially the $O_2/N_2$ data added to 1.1 times the $CO_2$ data. APO is an approximately conservative tracer with respect to the land biota.

[3] Global trends for the 1990s are calculated simply as the 1990.0 annual averages subtracted from the 2000.0 averages.

[4] Uses total moles of dry air equal to 1.769 x $10^{20}$, and an atmospheric $O_2$ mole fraction of 0.2095 [*Machta and Hughes*, 1970].

**Table 3.** Global Fossil Fuel Combustion Data for the 1990s

| Year | $CO_2$ produced[1] ($10^6$ tonnes)[2] | $O_2$ consumed[3] ($10^6$ tonnes) | $O_2$:C molar ratio |
|---|---|---|---|
| 1990 | 6,104 | 22,581 | 1.389 |
| 1991 | 6,183 | 22,955 | 1.394 |
| 1992 | 6,095 | 22,546 | 1.388 |
| 1993 | 6,073 | 22,514 | 1.391 |
| 1994 | 6,221 | 23,029 | 1.389 |
| 1995 | 6,407 | 23,752 | 1.392 |
| 1996 | 6,517 | 24,181 | 1.393 |
| 1997 | 6,601 | 24,517 | 1.394 |
| 1998 | 6,566 | 24,339 | |
| 1999 | 6,521 | 24,172 | |
| Total | 63,288 | 234,587 | 1.391[4] |
| Total ($10^{14}$ mol) | 52.70 | 73.32 | |

[1] Data are from *Marland et al.* [2000], and include $CO_2$ produced from solid, liquid, and gas fuel, as well as from flared gas and cement manufacture.

[2] $10^6$ tonnes is equivalent to 0.001 Gt, or 0.001 Pg.

[3] $O_2$ consumed is calculated assuming full combustion of all fossil fuel types, and using $O_2$:$CO_2$ molar ratios for each fuel type from *Keeling* [1988a]. That is, $O_2$:$CO_2$ is 1.17 for solid fuel; 1.44 for liquid fuel; 1.95 for gas fuel; and 1.98 for flared gas. (Cement manufacture does not consume $O_2$.)

[4] Average $O_2$:$CO_2$ molar ratio.

**Table 4.** Uncertainties in Global Land Biotic and Oceanic Sink Calculations

| Quantity | Value | Uncertainty | Source |
|---|---:|---:|---|
| $\alpha_B$ | 1.1 | ±0.05 | [*Severinghaus*, 1995] |
| $\alpha_F$ | 1.391 | ±0.04 | [*Keeling*, 1988a] |
| Fossil fuel emissions | 6.33 Gt C/y | ±0.38 Gt C/y | [*Marland et al.*, 2000] |
| $CO_2$ trend | 3.21 Gt C/y | ±0.13 Gt C/y | [*Tans et al.*, 1989; *Conway et al.*, 1994] |
| Oceanic $O_2$ degassing | $1.64 \times 10^{13}$ mol/y | $\pm 1.64 \times 10^{13}$ mol/y | This study |
| APO trend: | | | |
| - from "typical" trend calculation | | ±6 per meg | This study |
| - lack of southern hemisphere data | | ±3 per meg | This study |
| - additional La Jolla | | ±3.2 per meg | This study |
| - additional Alert | | ±3.4 per meg | This study |
| - total | -80.4 per meg | ±8.2 per meg | This study |

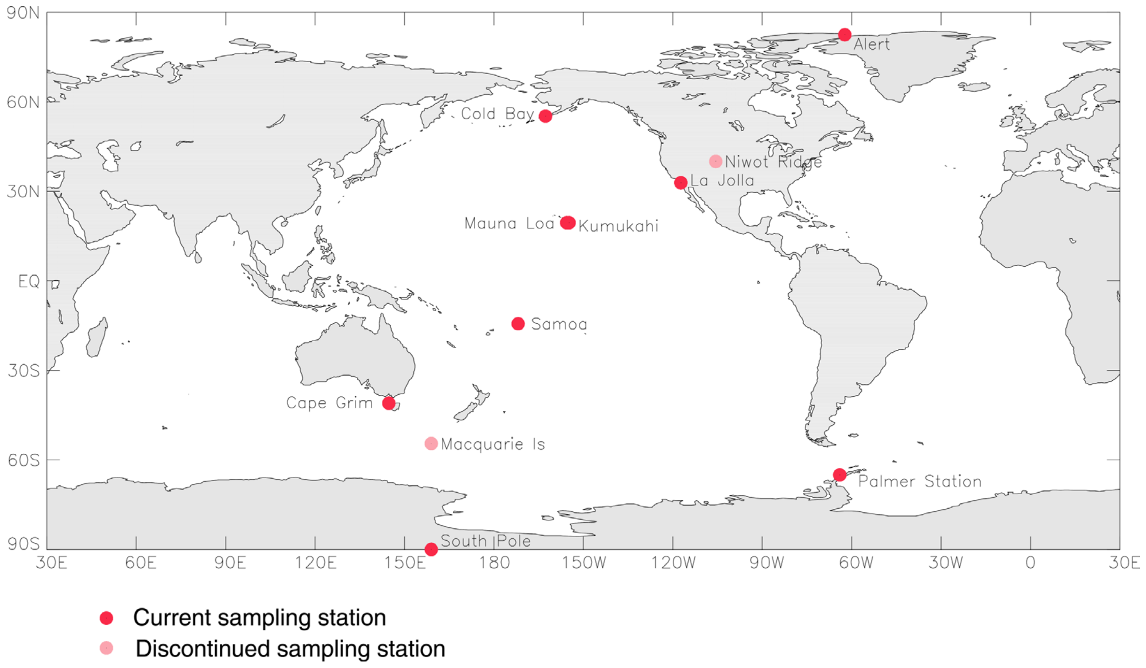
90N
60N
30N
EQ
30S
60S
90S
30E
60E
90E
120E
150E
180
150W
120W
90W
60W
30W
0
30E
Alert
Cold Bay
Niwot Ridge
La Jolla
Mauna Loa
Kumukahi
Samoa
Cape Grim
Macquarie Is
Palmer Station
South Pole
● Current sampling station
● Discontinued sampling station

**Figure 1.**

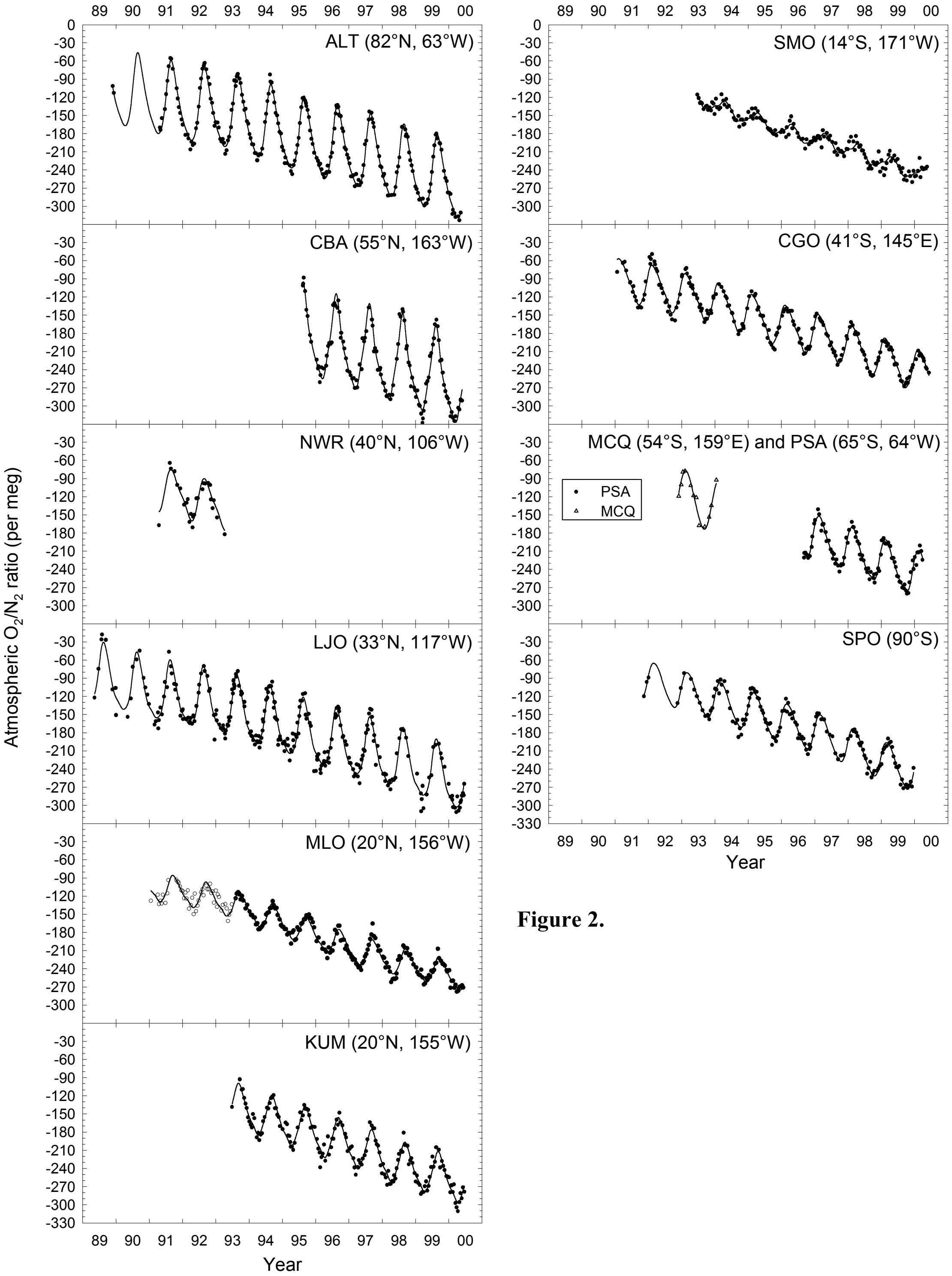
ALT (82°N, 63°W)
CBA (55°N, 163°W)
NWR (40°N, 106°W)
LJO (33°N, 117°W)
MLO (20°N, 156°W)
KUM (20°N, 155°W)
SMO (14°S, 171°W)
CGO (41°S, 145°E)
MCQ (54°S, 159°E) and PSA (65°S, 64°W)
PSA
MCQ
SPO (90°S)
Atmospheric $O_2/N_2$ ratio (per meg)
Year
89
90
91
92
93
94
95
96
97
98
99
00
0
-30
-60
-90
-120
-150
-180
-210
-240
-270
-300
-330

**Figure 2.**

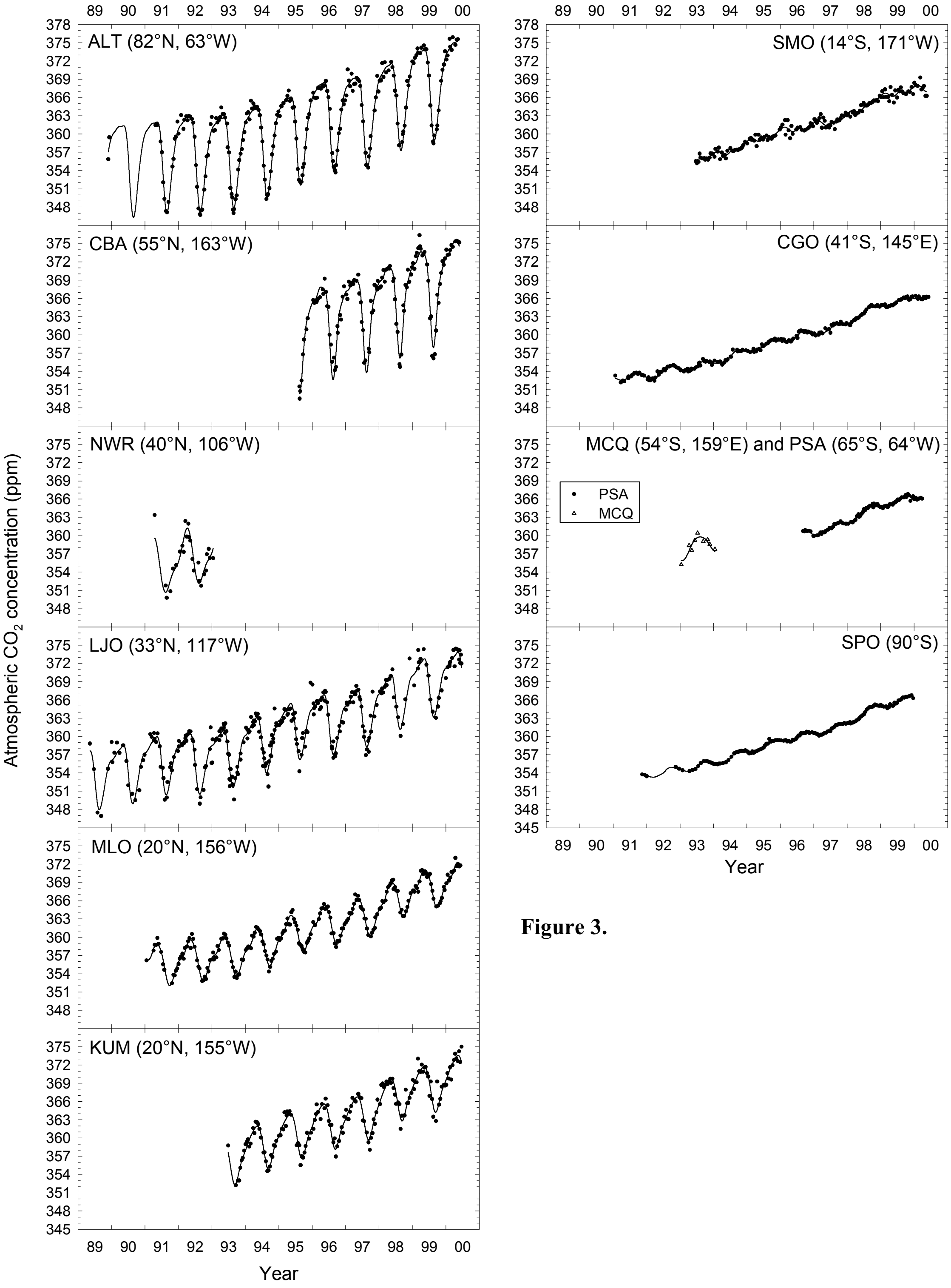
ALT (82°N, 63°W)
CBA (55°N, 163°W)
NWR (40°N, 106°W)
LJO (33°N, 117°W)
MLO (20°N, 156°W)
KUM (20°N, 155°W)
SMO (14°S, 171°W)
CGO (41°S, 145°E)
MCQ (54°S, 159°E) and PSA (65°S, 64°W)
SPO (90°S)
PSA
MCQ
Atmospheric $CO_2$ concentration (ppm)
Year
89
90
91
92
93
94
95
96
97
98
99
00
345
348
351
354
357
360
363
366
369
372
375
378

**Figure 3.**

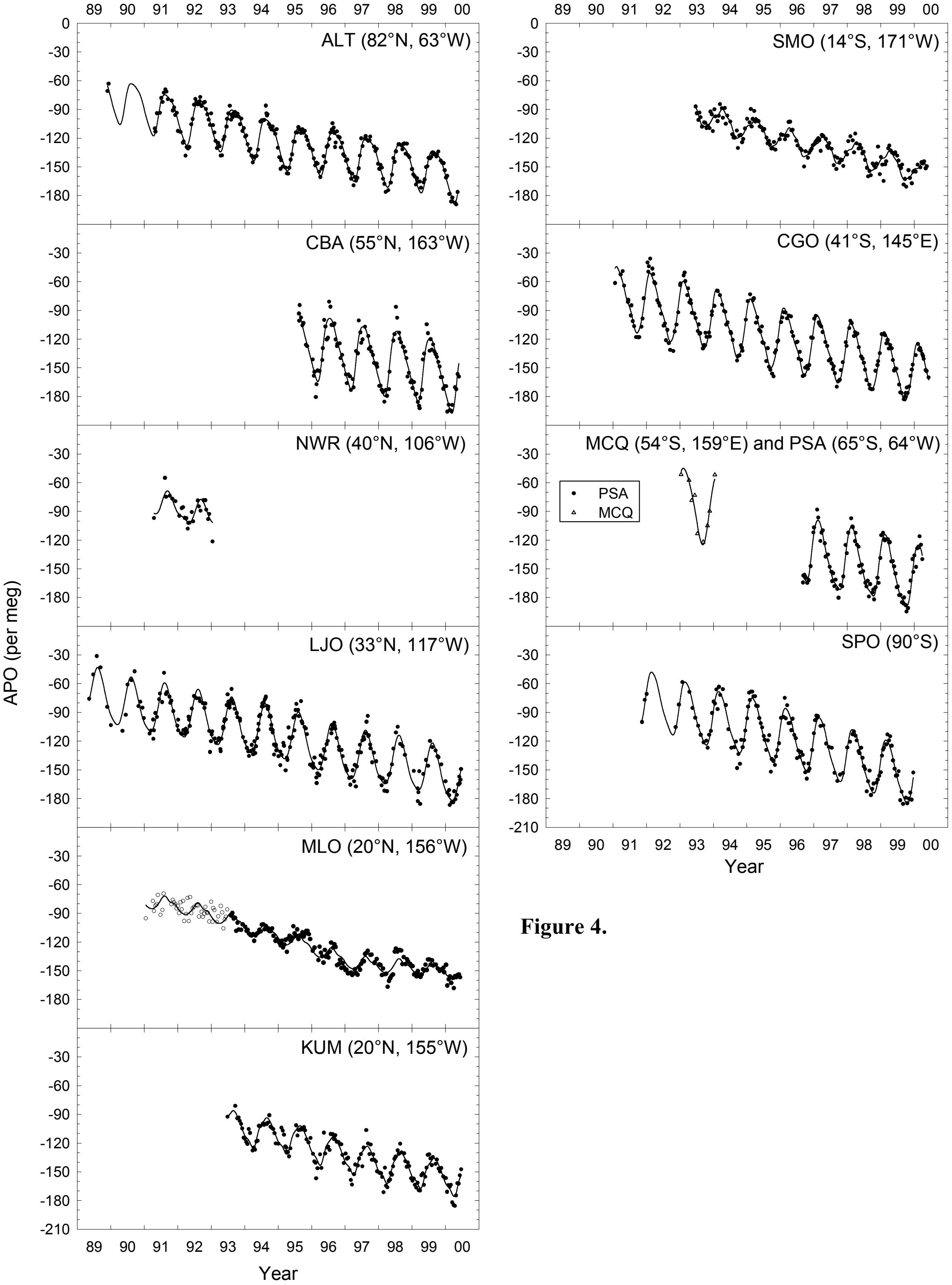

89
90
91
92
93
94
95
96
97
98
99
00
0
-30
-60
-90
-120
-150
-180
-210
ALT (82°N, 63°W)
CBA (55°N, 163°W)
NWR (40°N, 106°W)
LJO (33°N, 117°W)
MLO (20°N, 156°W)
KUM (20°N, 155°W)
SMO (14°S, 171°W)
CGO (41°S, 145°E)
MCQ (54°S, 159°E) and PSA (65°S, 64°W)
● PSA
△ MCQ
SPO (90°S)
APO (per meg)
Year

**Figure 4.**

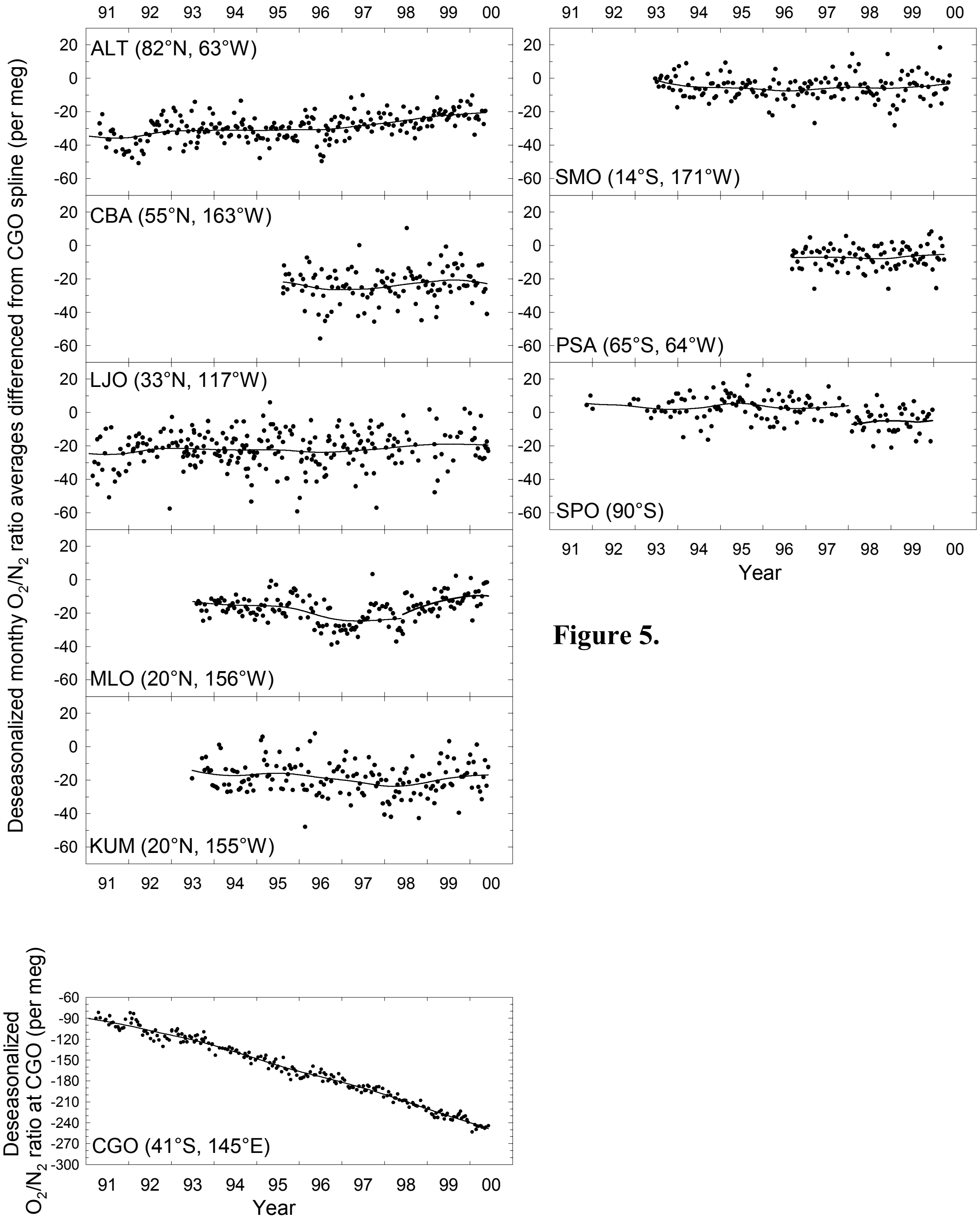

ALT (82°N, 63°W)
CBA (55°N, 163°W)
LJO (33°N, 117°W)
MLO (20°N, 156°W)
KUM (20°N, 155°W)
SMO (14°S, 171°W)
PSA (65°S, 64°W)
SPO (90°S)
CGO (41°S, 145°E)
Deseasonalized monthy O$_2$/N$_2$ ratio averages differenced from CGO spline (per meg)
Deseasonalized O$_2$/N$_2$ ratio at CGO (per meg)
20
0
-20
-40
-60
-90
-120
-150
-180
-210
-240
-270
-300
91
92
93
94
95
96
97
98
99
00
Year

**Figure 5.**

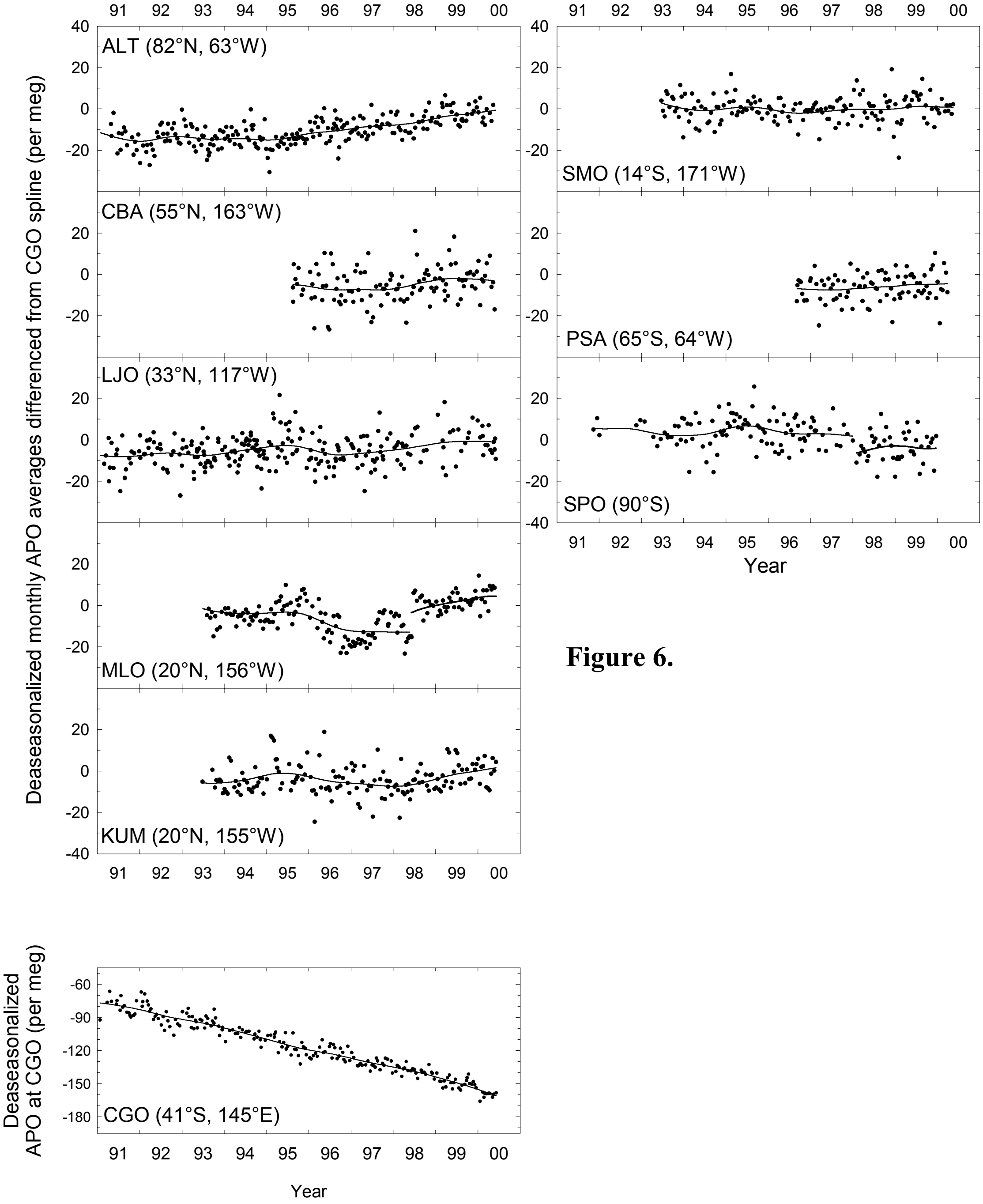

Deaseasonalized monthly APO averages differenced from CGO spline (per meg)
ALT (82°N, 63°W)
CBA (55°N, 163°W)
LJO (33°N, 117°W)
MLO (20°N, 156°W)
KUM (20°N, 155°W)
SMO (14°S, 171°W)
PSA (65°S, 64°W)
SPO (90°S)
40
20
0
-20
-40
91
92
93
94
95
96
97
98
99
00
Year
Deaseasonalized APO at CGO (per meg)
CGO (41°S, 145°E)
-60
-90
-120
-150
-180

**Figure 6.**

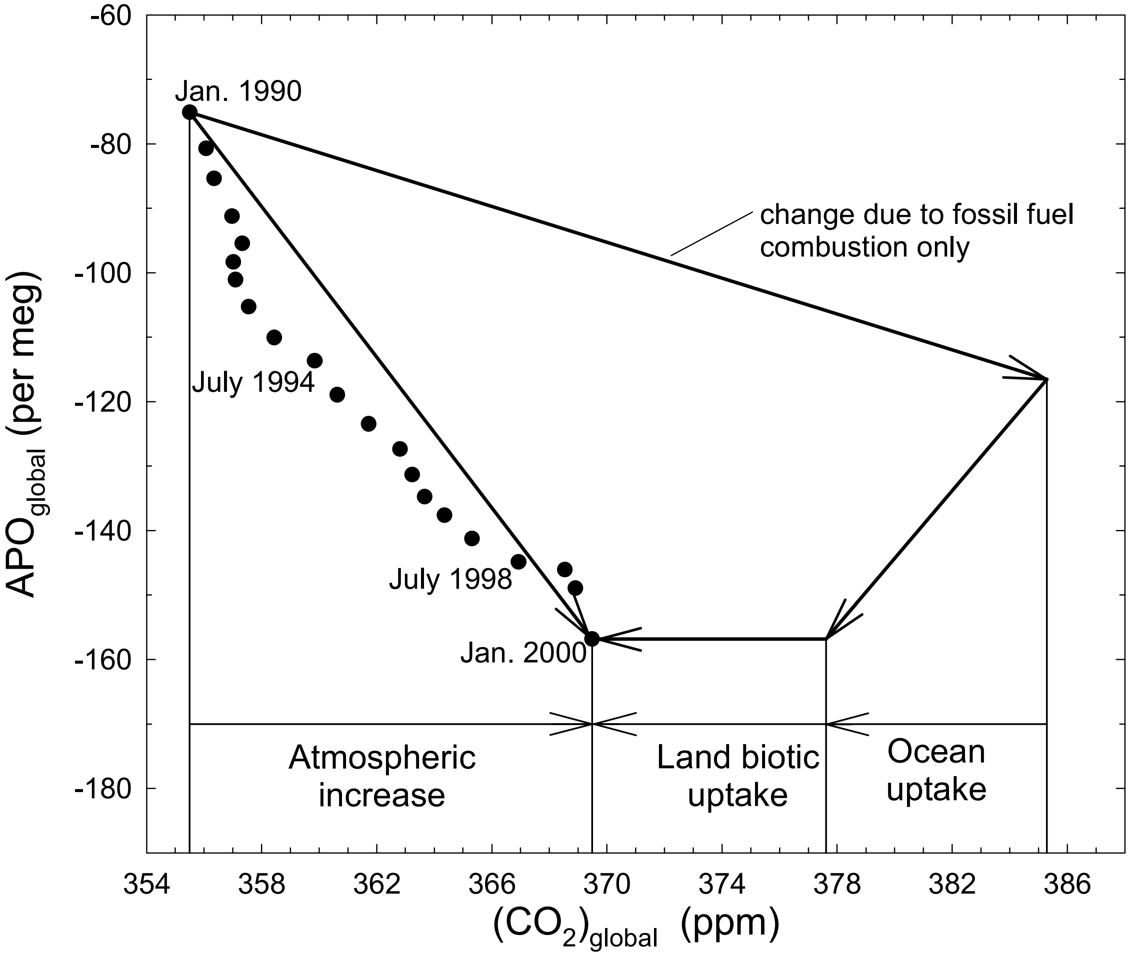

-60
-80
-100
-120
-140
-160
-180
APO$_{global}$ (per meg)
354
358
362
366
370
374
378
382
386
(CO$_2$)$_{global}$ (ppm)
Jan. 1990
July 1994
July 1998
Jan. 2000
change due to fossil fuel combustion only
Atmospheric increase
Land biotic uptake
Ocean uptake

**Figure 7.**

**Figure 8.**

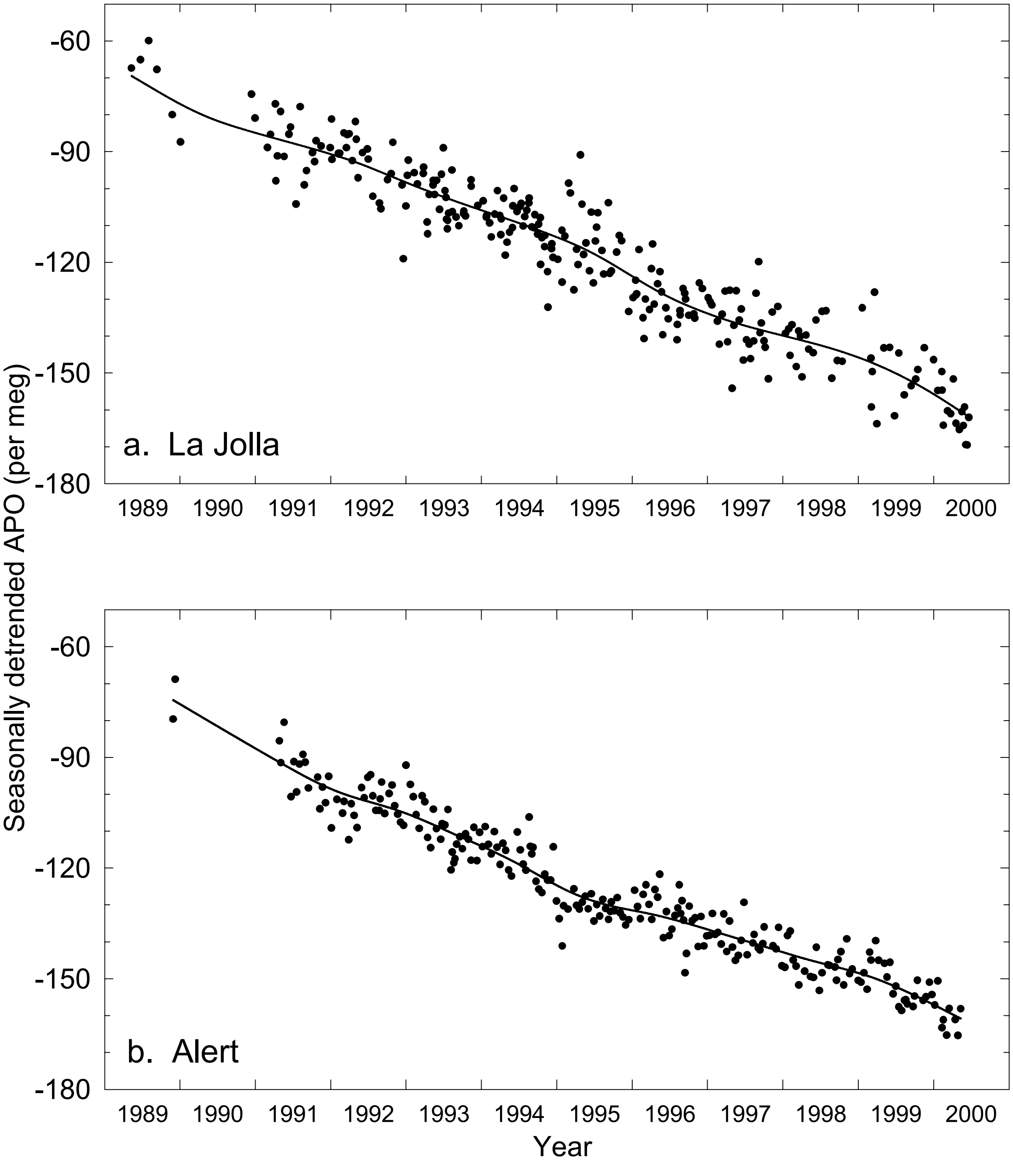
Seasonally detrended APO (per meg)
-60
-90
-120
-150
-180
a. La Jolla
1989
1990
1991
1992
1993
1994
1995
1996
1997
1998
1999
2000
-60
-90
-120
-150
-180
b. Alert
1989
1990
1991
1992
1993
1994
1995
1996
1997
1998
1999
2000
Year

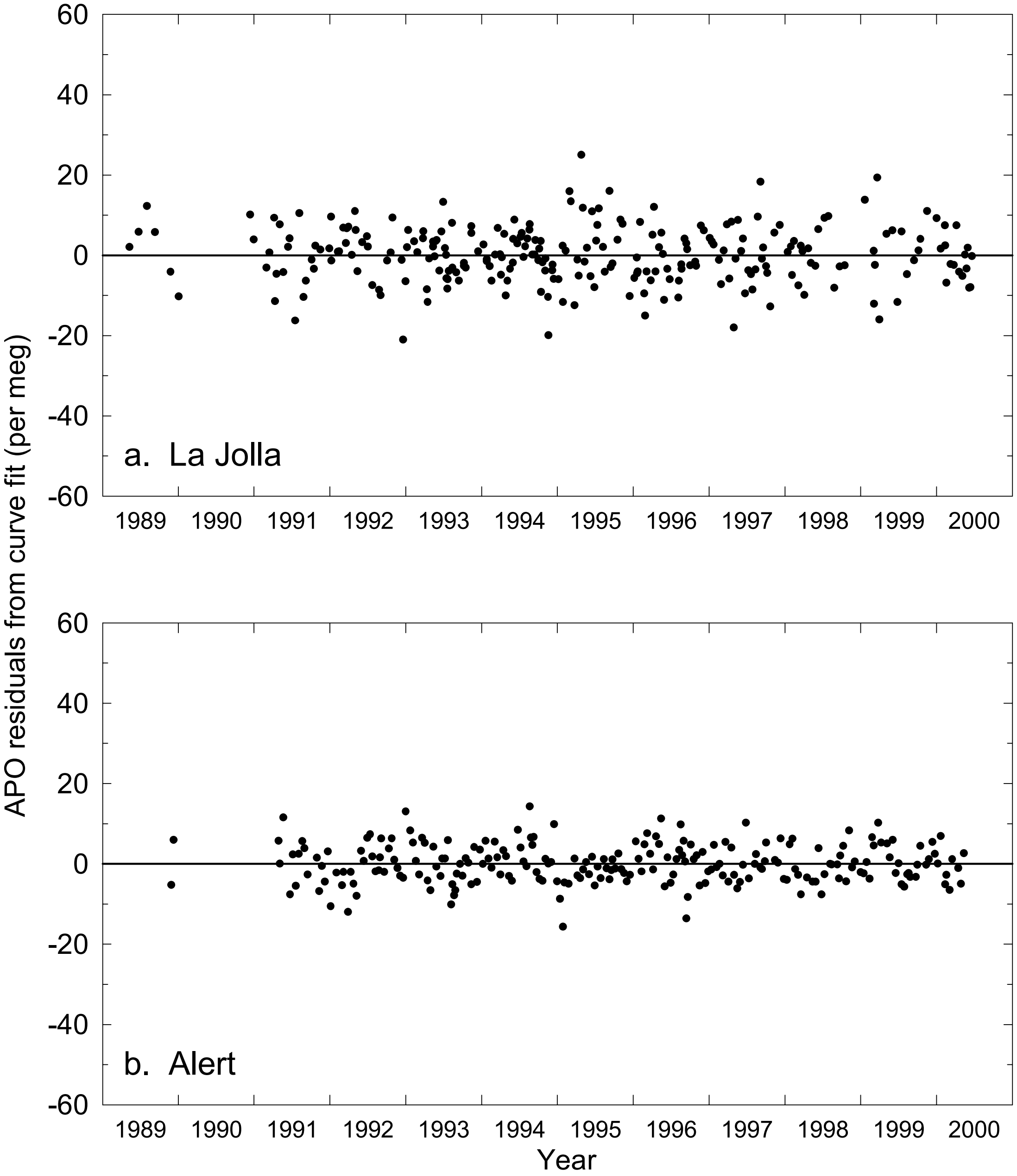
APO residuals from curve fit (per meg)
60
40
20
0
-20
-40
-60
a. La Jolla
b. Alert
1989
1990
1991
1992
1993
1994
1995
1996
1997
1998
1999
2000
Year

**Figure 9.**